The Second Generation Intact Stability Criteria: An Overview of Development

W. Peters (M), **V. Belenky** (M), **C. Bassler** (M), **K. Spyrou** (M), **N. Umeda** (M), **G. Bulian** (V), **B. Altmayer** (V)

This paper describes the current state of development of the second generation of International Maritime Organization (IMO) intact stability criteria. The objective of the paper is three-fold. First, it is a brief review of the recent history of related IMO development with emphasis on the question: why is the second generation of stability criteria needed? Second, the paper describes the framework of the new criteria in which they are complementary to the existing IMO criteria. The new criteria are applied only to those designs that may be susceptible to one of the modes of stability failure considered (parametric roll, pure loss of stability, surf-riding/ broaching). This is achieved through a set of formalized procedures of vulnerability checks. The ideas, proposals and justifications of these procedures represent the novel contents of the paper. Last, the paper reviews available technologies for development of direct stability assessment methods or performance-based criteria that should be available for those rare cases when susceptibility to these modes of failures is too high.

INTRODUCTION: REVIEW OF INTACT STABILITY DEVELOPMENTS AT IMO

The origin of the first-generation intact stability criteria that are included in the foundation of the International Code on Intact Stability, the 2008 IS Code (IMO, 2009) can be traced to the pioneering works of Rahola (1939), as well early versions of the weather criterion developed in the 1950s. The history of development and the background of these criteria are described by Kobylinski & Kastner (2003); a summary of the origin of these criteria is also available in chapter 3 of the Explanatory Notes to the International Code on Intact Stability (MSC.1/Circ.1281[1]).

The first generation intact stability criteria was originally codified at IMO in 1993 as a set of recommendations in Res. A.749(18) by taking into account, among other things, former Res. A.167(ES.IV) ("Recommendation on intact stability of passenger and cargo ships under 100 metres in length" which contained statistical criteria, heel due to passenger crowding, and heel due to turn, 1968) and Res. A.562(14) ("Recommendation on a severe wind and rolling criterion (Weather Criterion) for the intact stability of passenger and cargo ships of 24 metres in length and over," 1985). These criteria were codified in the 2008 IS Code and became effective as a part of both the SOLAS and International Load Line Conventions in 2010 (IMO Res. MSC.269(85) and MSC.270(85)).

The criteria in Part A of 2008 IS Code are based on a traditional empirical/statistical approach, with the exception of the Weather Criterion. The criteria for passenger vessels associated with heeling due to turn and the crowding of passengers to one side are formulated using a physics-based mathematical model of ship heeling.

The Weather Criterion is based upon a mathematical model of a ship heeling under the action of a sudden wind gust after being excited by regular waves and a steady wind. The parameters of the Weather Criterion were "tuned" using a sample population of ships, which limits the applicability of the Weather Criterion, in addition to the assumptions of the mathematical model used. In response to this, an alternative experimental approach for the Weather Criterion was also adopted by IMO (*cf.* MSC.1/Circ.1200 and MSC.1/Circ.1227).

The introduction of ships with characteristics and/or modes of operation which are significantly different from the reference population of ships on which the first generation criteria was based challenges the assumption that adequate intact stability is provided using the current criteria. A series of stability-related accidents in the last 15 years, involving ships such as the *APL China*, M/V *Aratere*, and *Chicago Express*, clearly demonstrates that intact stability criteria must be revisited.

The development of the second generation intact stability criteria started in 2002 with the re-establishment of the intact-stability working group by IMO's Subcommittee on Stability and Load Lines and on Fishing Vessels Safety (SLF) (*cf.* Francescutto, 2004, 2007). However, due mainly to the priority of revising the IS Code for approval, the actual work on the second generation intact stability criteria did not commence in earnest until the 48th session of the SLF in September 2005. The Working Group decided that the second generation intact stability criteria should be performance-based and address three modes of stability failure (SLF 48/21, paragraph 4.18):

- Restoring arm variation problems, such as parametric excitation and pure loss of stability;
- Stability under dead ship condition, as defined by SOLAS regulation II-1/3-8; and
- Maneuvering related problems in waves, such as broaching-to.

A similar formulation was included in the preamble of the 2008 IS Code, indicating the direction of the long-term development. However, the restoring arm variation problem was considered as two problems: modes of parametric roll and pure loss of stability; hence, four stability failure modes were considered.

During this initial development, there was general agreement that the second generation criteria should be based on the

[1] References to IMO documents such as "MSC.1/Circ.1281" appear in the list of references with an "IMO" prefix, *i.e.* as: IMO MSC.1/Circ.1281. As there is no ambiguity in the names of the IMO citations, the year will be omitted from the citations.

physics of the specific phenomena leading to stability failure. The design and modes of operation of new ships take on characteristics that cannot, with confidence, rely solely on the statistics of failures and regression-based methods. Also, there was general agreement on the desirability of relating the new criteria to probability, or some other measures of the likelihood of stability failure, as methods of risk analysis have gained greater acceptance and become standard tools in other industries (*e.g.* SLF 48/4/12).

These considerations led to the formulation of the framework for the second generation intact stability criteria, described in SLF 50/4/4 and discussed at the 50th session of SLF (May 2007). The key elements of this framework were the distinction between performance-based and parametric criteria, and between probabilistic and deterministic criteria. Special attention was paid to probabilistic criteria; the existence of the *problem of rarity* was recognized for the first time and a definition was offered. Also, due to the rarity of stability failures, the evaluation of the probability of failure with numerical tools was recognized as a significant challenge.

By that time (2007), there was already some experience in the maritime industry on how to handle some issues related to dynamic stability. Following a parametric roll accident on the *APL China* (France, *et al.*, 2003), the American Bureau of Shipping (ABS) issued a guide for the assessment of parametric roll for containerships (ABS, 2004). The guide was based on a multi-tiered assessment procedure. The first level—the susceptibility criteria, was built upon evaluation of changing GM in regular waves and the Mathieu equation. If the ship was found to be susceptible to parametric roll, then a more complex criterion was applied. This "severity" criterion involved the calculation of the full GZ curve in waves and numerical integration of the roll equation. If the roll response was "severe enough," then advanced numerical simulations were applied and ship-specific operational guidance was developed using a program such as the Large Amplitude Motion Program (LAMP) (Lin & Yue, 1990). While conservative, the susceptibility and severity criteria were still capable of identifying ships for which parametric roll was not possible.

Also at that time, the work of Germanischer Lloyd was focused on numerical assessment procedures using the advanced numerical code, GL Simbel (Brunswig & Pereira, 2006, Shigunov & Pereira, 2009). Furthermore, the Germanischer Lloyd development was focused on the preparation of ship-specific operational guidance for the avoidance of parametric roll (Shigunov, 2009).

Besides the efforts by classification societies, significant progress was achieved in developing training programs in order to increase crew awareness of parametric roll. An instructional video, produced by Herbert Engineering Corporation, is one successful example of this activity[1].

Analysis of these experiences led to an understanding that a multi-tiered approach should be applied for the development of the second generation intact stability criteria as a way to avoid unnecessary work. In view of this, the idea of vulnerability criteria was first formulated in the paper by Belenky, *et al.* (2008). The paper also gave a broad review of the physical background of the modes of dynamic stability failure considered. By virtue of its greater detail, this paper provided "explanatory notes" to SLF 50/4/4 and was submitted to the 51st session of SLF (SLF 51/INF.4) as additional information.

The framework of the second generation intact stability criteria took shape based on the work of the intersessional correspondence group (SLF 51/4/1 Annex 2). This document formalized the concepts contained in SLF 50/4/4; in particular, a clear distinction was made between a criterion and a standard, the former being "an instrument of judging," while the latter is a boundary between acceptable and unacceptable.

In 2005, the Japan Society of Naval Architects and Ocean Engineers (JASNAOE) established a Strategic Research Committee on Estimation Methods for Capsizing Risk for the IMO New Generation Stability Criteria (SCAPE Committee). The outcome of this program was reported in five sessions of JASNAOE; some other results were reported in English at the Osaka Colloquium (Ikeda, *et al.,* 2008). An overview of this work is available from SLF 51/INF.6. In the meantime, certain developments in the field were affected by the increasing consideration and practical formulation of the so-called "critical wave groups" approach. This was used for probabilistic intact stability assessment during the European SAFEDOR project *(e.g.* Themelis & Spyrou, 2007), which allowed for a practical interface between the deterministic and probabilistic viewpoints. SNAME established a Dynamic Stability Task Group whose purpose is to provide a detailed review of developments in the field of dynamic stability (SLF 53/3/3).

Vulnerability criteria were the focus of the 1st and 2nd International Workshops on Dynamic Stability Consideration in Ship Design (DSCSD) (Kobylinski, 2009).

The development of the second generation intact stability criteria was intensively discussed during the 10th International Conference on Stability of Ship and Ocean Vehicles and in the following 11th and 12th International Ship Stability Workshops (Degtyarev, 2009; van Walree, 2010; Belenky, 2011). In particular, a review was presented that examined the suitability of methods for vulnerability criteria (Bassler, *et al.*, 2009).

The consideration of excessive accelerations was also recently added to the list of stability failure modes (SLF 53/19, paragraph 3.28) following the partial stability failure of *Chicago Express*, which resulted in crew injuries and loss of life (BSU, 2009). While, technically, this issue is well-known, it has not yet been included in the regulatory framework. In a recent study, Shigunov *et al.* (2011) considered a vulnerability check for excessive accelerations based on initial GM and roll damping.

These discussions and developments were formed into proposals presented and discussed at the 52nd and 53rd sessions of SLF; (cf. SLF 52/3/1, SLF 52/INF.2, SLF 53/3/1, SLF 53/3/7, SLF 53/3/8, SLF53/3/9, SLF 53/INF.8, SLF 53/INF.10).

[1] Trailer available from www.herbert.com/videos/ParametricRoll/

THE CONCEPT OF THE SECOND GENERATION INTACT STABILITY CRITERIA

The assessment of dynamic stability in realistic wave conditions is a formidable task. The 2008 IS Code recognized this:

> *"In particular, the safety of a ship in a seaway involves complex hydrodynamic phenomena which up to now have not been fully investigated and understood. Motion of ships in a seaway should be treated as a dynamical system and relationships between ship and environmental conditions such as wave and wind excitations are recognized as extremely important elements. Based on hydrodynamic aspects and stability analysis of a ship in a seaway, stability criteria development poses complex problems that require further research."*

A realistic seaway is also random, *i.e.* described as a stochastic process; therefore, the problem must also be considered in a probabilistic context. Further, the occurrence of of stability failure (a random event) is rare—such that the natural period of roll can be considered as infinitely small in comparison with the expected time before such an event.

The existence of the problem of rarity makes direct, brute-force numerical simulation impractical for the evaluation of dynamic stability failure. There are special procedures that allow the problem of rarity to be addressed, which are discussed later in this paper. However, the solution may include numerical simulations using hydrodynamic codes (such as LAMP[1], FREDYN[2], GL-SIMBEL[3], TEMPEST[4], and others), hybrid codes (such as CAPSIM[5], LAIDYN[6], SHIXDOF[7], SIMCAP[8], and others) or simpler ordinary differential equation (ODE) tools (such as OU BROACH[9], ROLLS[10], and others). Preparing input data for these tools may include model testing. While these tools represent the current state of the art (*cf.* Beck & Reed, 2001), their application is expensive and requires proper justification of the necessity of their application, because not all ships are vulnerable to these stability failures.

This justification can be completed in the form of a multi-tiered approach (see Figure 1), whereby a ship would be checked for vulnerability in the first tiers and, if found vulnerable, then the ship would be evaluated using state-of-the art direct stability assessment methods. Taking into account the intended regulatory application, two tiers of vulnerability criteria would be applied. The first level is meant to be very simple and conservative. Its main purpose is to distinguish ships (and the loading conditions) that clearly are not vulnerable to a given stability failure mode, from those that, in principle, may be. Because further analysis of the vessels that are not vulnerable would be redundant, the cost of performing such further analysis should be avoided.

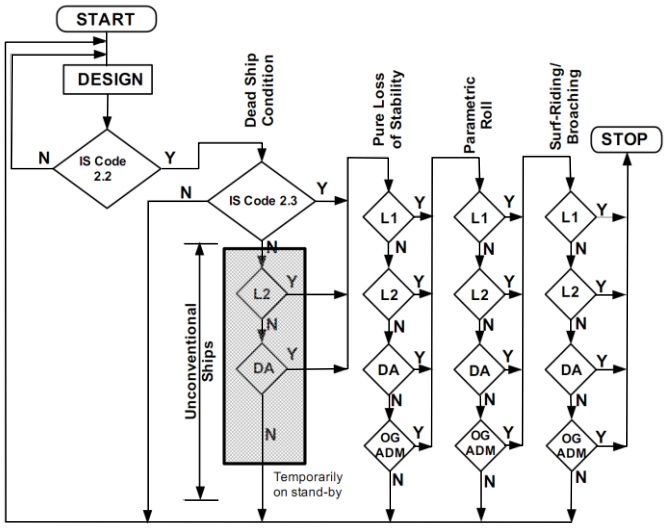

Figure 1. Multi-tiered Approach for the Second Generation Intact Stability Criteria (SLF53/WP.4 Annex 3)

As an example, very large crude carriers are wall-sided for the most of the length of the hull and, therefore, cannot experience significant stability changes in waves. Therefore, this type of ship is not expected to be vulnerable to the righting-lever variation problems of either parametric roll or pure loss of stability. By basing the first-level vulnerability criteria on the geometry characteristics of the hull and speed, rather than the ship type per se, an easy first assessment of vulnerability may be made. Therefore, the criteria will remain valid for any novel ship design.

Because the level-one criteria are to be simple and conservative, some occasional "false positives" may be expected. Again, to reduce the time and cost of stability assessment, a second level of vulnerability criteria is introduced. The second level is meant to be less conservative than the first, based on simplified physics and involving calculations with reduced computational efforts and straightforward applications following suitable guidelines.

There has been very active development of the vulnerability criteria over the past two years. While this work has not been completed, significant progress has been made since 2009, when a review of eligible methods was prepared (Bassler, *et al.*, 2009). The next three sections of this paper describe these ideas, their technical justification and sample calculations.

VULNERABILITY CRITERIA FOR PURE LOSS OF STABILITY

Physical Background: Changing Stability in Waves

When a ship is sailing through waves, the submerged portion of the hull changes. These changes may become especially significant if the length of the wave is comparable to the length of the ship. For example, let us examine the changes that occur when the trough of a wave is located amidships, applicable for the most monohull vessels (see Figure 2a). The upper part of

[1] Lin & Yue (1990); [2] de Kat, *et al.* (1994); [3] Pereira (1988); [4] Belknap & Reed (2010); [5] Spanos & Papanikolaou (2006); [6] Matusiak (2000); [7] Bulian & Francescutto (2008); [8] Schreuder (2005); [9] Hashimoto, *et al.* (2011); [10] Söding (1982)

the bow section is usually wide, due to bow flare, which makes the waterplane larger if the upper part of the bow section is partially submerged. The upper part of the aft section is even larger than the bow section; thus the aft part of the waterplane becomes larger once the upper part of the aft section is submerged. Unlike the bow and aft sections, the midship section is wall-sided for most displacement hulls. This means that very little change occurs in the waterplane width with draft—when the wave trough is amidships, the draft at the midship section is low, but the waterplane does not change much. As a result, when the wave trough is around the midship section, the waterplane is larger than it is in calm water.

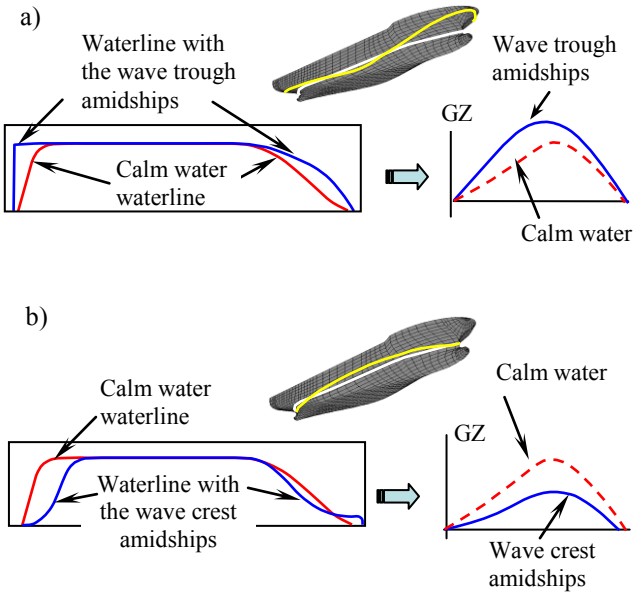

Figure 2. Change of Stability in Waves; a) on Wave Trough b) on Wave Crest

When the wave crest is located around the midship section, the situation changes dramatically, see Figure 2b. When the wave crest is located amidships, a wave trough is located near the fore and aft sections. The underwater part of the bow section is usually quite narrow, especially around the waterline and the underwater part of the aft section is also very narrow. Thus when troughs are fore and aft, the draft at the bow and the stern becomes shallow, which makes the waterplane very narrow.

As is well known from ship hydrostatics, the waterplane area has a significant effect on ship stability because it is directly related to the inertia of the waterplane. If the waterplane loses area, then the GZ curve is also reduced.

Pure loss of stability is related to prolonged reduction of the GZ curve on (or near) the wave crest. This situation occurs in following and stern-quartering seas when the ship speed is close to the wave celerity. If an additional heeling (or rolling) moment (e.g. lateral gusty wind load, short-crested wave effect or centrifugal force due to course keeping) is applied, a ship may attain a large roll angle and even capsize.

Level 1 Vulnerability Criteria for Pure Loss of Stability

Some hulls are more prone to pure loss of stability than others. A hull with large freeboard and significant change of geometry in the fore and aft sections, but with a small GM value, may suffer from significant loll angle due to deterioration of stability on the wave crest. As can be seen from Figure 3, loll angles resulted in large angles of heel when the wave crest was passing near the midship section

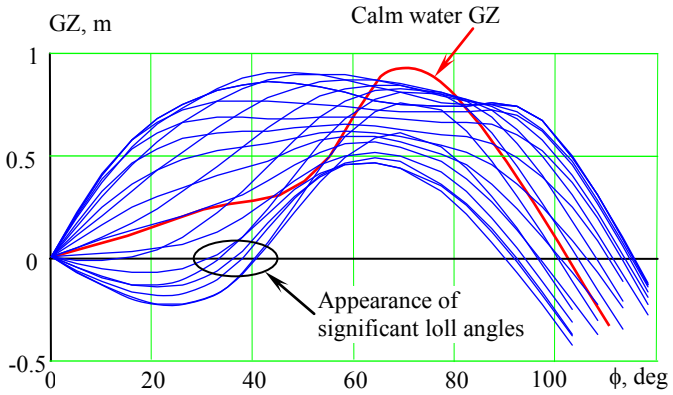

Figure 3 Wave Passing Effect on GZ Curve of a RoPax Ship in IMO-critical Loading Conditions

Pure loss of stability is driven by stability changes in longitudinal waves. As discussed above, certain features of the hull shape are "responsible" for stability change. One of the possible options proposed for the Level 1 Criterion is focused on these geometric features (SLF 53/INF.10 Annex 5).

The criterion is the average value of the vertical wall-sidedness coefficients for the fore and aft quarter portions of the hull, both above and below the waterline. The coefficient for vertical "wall-sidedness," C_{VWS}, measures the variation of the fore or aft quarter of the waterplane area, either from the base line to the design draft or from the design draft up to the shear line (see Figure 4). The threshold value as the standard should be determined from sample calculations.

The coefficient is taken relative to the maximum waterplane area of the fore or aft portion over the specified range of drafts,

$$C_{CWS}^{below} = \frac{\int_0^d A_{WP}(z)dz}{\max(A_{WP}(z))\cdot d}, \qquad C_{CWS}^{above} = \frac{\int_d^D A_{WP}(z)dz}{\max(A_{WP}(z))\cdot (D-d)}, \tag{1}$$

where d is draft, D is depth, and A_{WP} is waterplane area of fore or after quarter of the waterplane.

The second proposed option considered is a conditional value of minimum GM calculated as follows (SLF 53/INF.10 Annex 2):

$$GM_{\min} = KB + \frac{I_L}{V} - KG \quad (2)$$

where KB is the distance of the center of buoyancy from the base line, V is the volumetric displacement calculated for the design draft, and KG is the distance from the base line to the center of gravity in design-loading conditions. I_L is the moment of inertia of the water plane calculated for a fraction of the draft, which normally should be determined as the intersection between the flat of side and the bilge radius at amidships. Since the waterplane breadth in the midship section is almost unchanged, the waterplane area on the wave crest can be approximated with that in calm water but with the smallest draft. As a result, the required value of I_L can be taken from an existing hydrostatic table so that no additional calculations using hull geometry are required. In this case, the threshold value as the standard can be regarded as zero. Another advantage of the criterion is its potential ability to differentiate between multiple loading conditions.

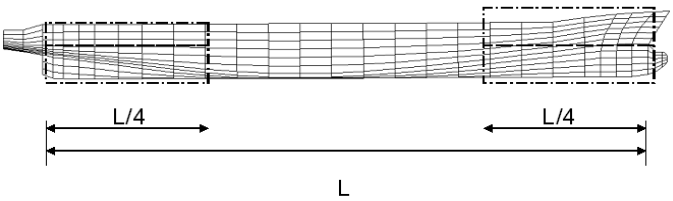

Figure 4 Notional Ship Profile with the Four Portions of the C_{VWS} Considered for the Level 1 Vulnerability Assessment

Both criteria are based on understanding that the vertical variability of the hull shape at bow and stern, but not at the midship section, is responsible for stability changes in waves. The results of calculations for 40 sample ships are presented in Tables 1 and 2. The value 0.8 was considered as a tentative standard for the criterion (1) in SLF 53/INF.10 Annex 5, while $GM_{\min}>0$ was proposed in the Annex 2 of SLF 53/INF.10

Preliminary analysis needs be done while criteria (1) and (2) are still considered "draft" (as well as all other criteria considered in this paper). First, the criteria (1) and (2) seem to agree for most of the cases considered. The only exceptions are the two multi-purpose vessels (MPVs) (L = 135 m and 105 m), the 5500 DWT bulk carrier, the 110 m tanker and both tugs.

The ONR flared topside configuration (Naval Combatant 1) represents the hull shape of a notional conventional destroyer. The extensive operational experience of conventional destroyer hulls shows that they are not known for any pure loss of stability failures. Therefore, both criteria are conservative in this case because the hull shape causes significant change of waterplane area, while the KG-value is low enough to compensate for degradation of stability in a wave crest. Similar situations can be observed for the Japanese Purse Seiner, the small tanker (L = 110 m), the 105 m MPV and both tugs.

The situation with the 135 m MPV and the 5500 DWT bulk carrier seems to be the opposite: the change of water-plane area is not dramatic, but the reserve KG may be insufficient to counter the decrease of stability on a wave crest.

Table 1 Sample Calculations on Pure Loss based on Ships from SLF 53/INF.10 Annex 5

Ship	**Description**	***L*, m**	***Cvwp*2**	***GM***	GM_{min}
Bulk Carrier 1		275	0.89	6.32	4.03
Bulk Carrier 2		145	0.87	1.53	0.27
Containership 1	Post-panamax	322.6	0.73	1.30	-6.23
Containership 2	Post-panamax	376	0.74	1.84	-6.23
Containership 3	Post-panamax	330	0.73	2.08	-3.08
Containership 4	Panamax	283.2	0.73	0.46	-4.01
Containership 5	C11 Class	262	0.67	1.9	-3.01
Fishing Vessel 1	Japanese Purse Seiner	34.5	0.68	1.00	-0.84
Fishing Vessel 2		21.56	0.69	0.73	-0.19
General Cargo 1	Series 60 C_B = 0.7	121.9	0.84	0.75	0.04
General Cargo 2	C4 Class	161.2	0.76	1.10	-0.53
LNG Carrier		267.8	0.85	3.40	0.34
Naval Combatant 1	ONR Flared	150	0.74	1.08	-1.75
Naval Combatant 2	ONR Tumblehome	150	0.71	2.06	-0.77
Passenger Ship		276.4	0.71	3.70	-0.49
RoPax		137	0.67	1.76	-0.58
Tanker		320	0.89	9.85	6.76

Both criteria unanimously exclude from vulnerability large tankers and the rest of the bulk-carriers; this exclusion does not require any comment as these ship types have never suffered from pure loss of stability. Both criteria detect vulnerability to pure loss of stability for both RoPax ships and the ONR Tumblehome topside hull form (Naval Combatant 2) for which vulnerability to pure loss of stability seems to be plausible, as these types of ships are known for such failures (Maritime New Zealand, 2007; Hashimoto, 2009).

Both criteria detect vulnerability to pure loss of stability for all the tested container carriers. This seems to be result of dramatic changes of the waterplane area for which containerships are known. It is also known that these changes are capable of causing parametric resonance, but not necessarily pure loss of stability. The Level 2 Vulnerability Criterion, then, is expected to be tested against this fact.

In general, it seems that criteria (1) and (2) complement each other; criterion (1) offers better accounting for the details of ship hull shapes, while criterion (2) provides a value that is specific for a given loading condition. Choice of the appropriate set of loading conditions remains to be done, as well as tuning computational parameters.

Level 2 Vulnerability Criteria for Pure Loss of Stability

As a first approximation, pure loss of stability may be considered as a single wave event because the changes in stability are instantaneous and do not have a memory. Typically, the worst-case wavelength is close to the length of the ship, $\lambda/L \approx 1.0$. However, in order to account for the effect of ship size relative to wave conditions, righting lever variations must be evaluated in irregular waves.

An irregular seaway can be presented as a series of encounters with sinusoidal waves with random length or wave number (spatial frequency) and height or amplitude. A joint distribution of these quantities is available from Longuet-Higgins (1957, 1976, 1984), which is based on the theory of an envelope of stochastic process (Rice, 1944/45). Based on Longuet-Higgins, each wave encounter can be associated with a statistical weight:

$$W_{ij} = \int_{a_i-\Delta a}^{a_i+\Delta a} \int_{k_j-\Delta k}^{k_j+\Delta k} f(a,k)\,dk\,da \qquad (3)$$

where a_i and k_i are amplitudes and wave numbers presented with a certain discretization over the probability density function:

Table 2 Sample Calculations on Pure Loss based on Ships from SLF 53/INF.10 Annex 9

Ship	Description	*L, m*	*Cvwp2*	*GM*	GM_{min}
Bulk Carrier	5500 DWT	190	0.79	2.84	1.91
Bulk Carrier		180	0.8	2.10	1.17
Containership	> 10000 TEU	360	0.75	0.80	-3.88
Containership	> 10000 TEU	360	0.76	0.7	-3.96
Containership	> 6000 TEU	320	0.74	0.70	-3.174
Containership	> 6000 TEU	320	0.73	0.80	-2.88
Containership	> 4000 TEU	250	0.7	0.5	-2.14
Containership	> 4000 TEU	250	0.71	0.6	-2.09
Containership	> 1000 TEU	210	0.71	0.60	-2.22
Containership	> 1000 TEU	200	0.7	0.60	-1.98
Containership	> 1000 TEU	170	0.69	0.5	-2.17
Containership	> 1000 TEU	160	0.7	0.16	-1.16
Containership	> 500 TEU	135	0.68	0.58	-1.00
Containership	> 500 TEU	125	0.67	0.70	-1.16
Cruise Vessel		240	0.76	2.71	-1.05
LNG Carrier	1000 cbm	110	0.74	1.06	-0.11
MPV		135	0.83	0.65	-0.05
MPV		125	0.8	0.17	-0.53
MPV		120	0.71	1.00	-0.33
MPV	7500 DWT	105	0.81	0.70	-0.01
Tanker	30000 DWT	320	0.83	6.35	4.69
Tanker		110	0.72	1.31	0.6
Tug		30	0.73	2.23	0.69
Tug		25	0.67	3.60	2.01

$$f(a,k) = f(a)f(k \mid a) = \frac{a^2}{\sqrt{k_2^2 - k_1^2}\sqrt{2\pi V_W^3}} \exp\left(-\frac{a^2}{2V_W}\right)$$
$$\times \left\{ \exp\left(-\frac{a^2}{2V_W}\frac{(k-k_1)^2}{(k_2^2-k_1^2)}\right) + \exp\left(-\frac{a^2}{2V_W}\frac{(k+k_1)^2}{(k_2^2-k_1^2)}\right)\right\},$$

where V_W is the variance of the wave elevations, k_1 is the mean wave number and k_2 is related to the mean width of spectrum s(ω) expressed in terms of wave numbers using the dispersion relation:

$$k_1 = \frac{1}{V_W}\int_0^\infty \frac{\omega^2}{g} s(\omega) d\omega;$$
$$k_2 = \sqrt{\frac{1}{V_W}\int_0^\infty \frac{\omega^4}{g^2} s(\omega) d\omega}.$$

The value of k_2 includes a fourth spectral moment. Not all approximations for sea spectra allow straightforward calculation of the fourth moment. It is known that calculations of the fourth moment for Bretschneider-type spectra are only possible if the frequency range is limited (Bishop & Price, 1978; St. Denis, 1980).

The criterion formulated for a regular wave relates wave length and height to a measure of deterioration of stability, while this wave passes the ship. Then the criterion for irregular waves can be sought as a mean value of a deterministic function of random variables: wave number and wave amplitude.

$$Ci = \sum_i \sum_j Cr(a_i, k_j) W_{ij}$$

where Cr is the criterion for a regular wave characterized with the wave number, k, and amplitude, a, while Ci is the same criterion averaged for irregular waves defined using a given spectrum.

Alternatively, the 2nd level vulnerability check can be done using just a series of regular waves systematically covering the entire range of possible steepness values. Here, the wavelength is assumed to be equal to the ship length as the worst-case scenario, while the range of steepness values remains to be determined.

Three criteria for regular waves are considered below. The first criterion is based on time duration while stability is degraded due to the passing wave.

The time while stability is decreased can be easily found if the instantaneous *GM* is considered a function of the wave crest position. To evaluate this function, the instantaneous *GM* is calculated on a series of wave water planes corresponding to different positions of the wave crest relative to the midship section (see Figure 5). Points $x1$ and $x2$ (Figure 6) show the distance when the *GM* remains below a critical level while the wave passes the ship.

The "time -below-critical GM", *tbc*, can be calculated as:

$$tbc = \frac{x2 - x1}{|c - V_S|} \quad (4)$$

where c is wave celerity and V_s is ship speed. The time-below-critical *GM* is a random number in irregular waves. Its mean value is estimated as:

$$m(tbc) = \sum_i \sum_j tbc_{ij} W_{ij}$$

Obviously, waves that produce celerity that is too close to ship speed must be excluded to avoid the singularity in Equation (4). The criterion value $Cr1$ is proposed as the following ratio:

$$Cr1 = \frac{m(tbc)}{T_\phi}, \quad (5)$$

where T_ϕ is a time scale of roll motions (not necessarily the period in calm water).

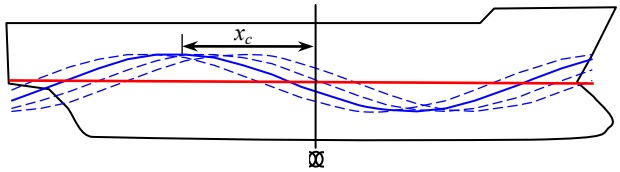

Figure 5. On Calculation of the Instantaneous GM in Waves

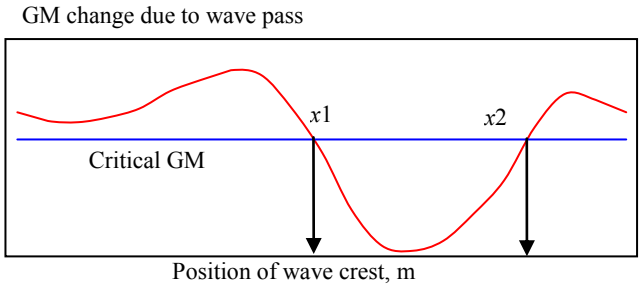

Figure 6. Calculation of "Time-Below-Critical-GM"

This criterion assesses the significance of stability changes in waves. If stability is degraded only for a short duration, this degradation may not be significant. However, for longer durations of decreased stability below the critical level, the restoring moment may be degraded enough to result in a dangerously large roll angle. More details on this criterion as well as sample calculations on notional naval ships is available from Belenky & Bassler (2010). This criterion may be further refined by including a simple model for surging, as the surge motion affects phases and therefore may change the timing.

The second criterion, *Cr2*, is set to detect if there are significant durations of negative *GM* (Figure 7). Appearance of an angle of loll may lead to the development of partial stability failure sooner, as the upright equilibrium is no longer stable. It is quite possible that some ships may be more vulnerable to these types of failure than others.

The second criterion is based on the time during which the angle of loll exceeds a certain limit angle, ϕ_{lim}. The time while the angle of loll is too large during the wave pass is expressed as:

$$tbz = \sum_k z_k \Delta t,$$

where value, z_k is an indicator, Δt is the time-step and index k corresponds to a particular time instant during the wave pass. For the k-th position of the wave crest along the hull crest, the indicator value, z_k, is calculated as:

$$z_k = \begin{cases} 0 if \, \phi_{loll} < \phi_{\lim} \\ 1 if \, \phi_{loll} \geq \phi_{\lim} \end{cases}.$$

(30 degrees was used as ϕ_{lim} in this example). Obviously, the angle of loll, ϕ_{loll}, can only be obtained from the *GZ* curve in waves. Calculations of the instantaneous *GZ* curve in waves are done in the same way as described for the instantaneous *GM* (Paulling, 1961). Since the encounter frequency is low, the influence of heave and pitch can be approximated quasi-statically through balancing trim and draft. Sometimes the GZ in waves can be approximated by using a calm-water *GZ* curve and the instantaneous *GM* in waves. However, caution has to be exercised as there are known cases when such approximations are not conservative (Annex 9, SLF 53/INF.10).

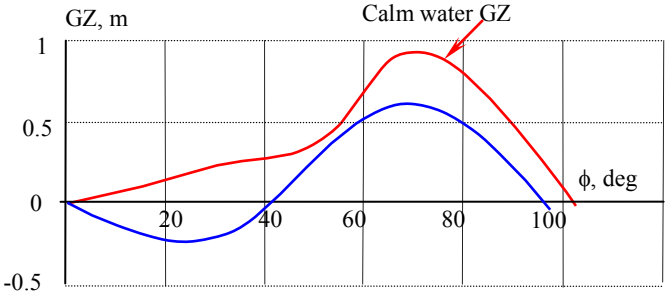

Figure 7 Deterioration of GZ Curve near the Wave Crest

Formulation of the second criterion is similar to the first one:

$$Cr2 = \frac{m(tbz)}{T_\varphi}, \qquad (6)$$

where T_ϕ is the chosen time scale, and $m(tbz)$ is the weighted average over the wave encounters:

$$m(tbz) = \sum_i \sum_j tbz_{ij} W_{ij}.$$

The third proposed criterion is based on the maximum of the GZ curve in waves. The suggested standard is zero, so the ship is considered to be vulnerable if the GZ curve becomes completely negative at least once during the series of calculations:

$$Cr3 = \min\left(GZ_{\max}(x_c, a, k)\right) < 0 \qquad (7)$$

Sample calculations for the criteria (5), (6), and (7) can be found in Annexes 2 and 5 of SLF 53/INF.10.

VULNERABILITY CRITERIA FOR PARAMETRIC ROLL

Physical Background: Parametric Resonance Caused by Changing Stability in Waves

The occurrence of parametric roll is caused by time-dependent stability changes. Typically, though not necessarily, the worst-case condition occurs when the encounter frequency between the ship and the wave is about twice the roll natural frequency. In some cases, the condition when the encounter frequency is close to the roll natural frequency can also be dangerous. The possibility of development of instability due to GZ curve changes in waves has been known since the 1930's (Watanabe, 1934, Kempf, 1938; Graff & Heckscher, 1941; Paulling & Rosenberg, 1959).

If the ship has a non-zero roll angle while in the wave trough, increased stability provides it a strong restoring force (i.e., pushback). As the ship returns to the upright position, its roll rate is greater since there was an additional pushback due to the increased stability. If at that time, the ship has the wave crest at midship, the stability is decreased and the ship will roll further to the opposite side because of the greater speed (i.e. inertia) of rolling and less resistance to heeling. Then, if the wave trough reaches the midship section when the ship reaches its maximum roll amplitude, stability increases and the cycle starts again. An important point is that there was one half of the roll cycle associated with the passing of an entire wave. So, there are two waves that pass per each roll period. That means the roll period is about twice that of the wave period, (Figure 8).

Even from this brief description, it is clear that for development of parametric roll, two conditions are needed: a variation of stability in waves and a certain ratio of encounter and natural frequency.

Level 1: Vulnerability Criteria for Parametric Roll

As the Level 1 vulnerability criteria for parametric roll is expected to be simple, it makes sense to use the Mathieu equation (the simplest model of parametric resonance) as the basis for the criteria. The linear roll equation with periodically changing *GM* can be transformed into the Mathieu equation:

$$(I_x + A_{44})\ddot{\phi} + B_{44}\dot{\phi} + W \cdot GM(t)\phi = 0 \qquad (8)$$

where I_x is the transverse moment of inertia, A_{44} is the added mass in roll B_{44} is the linear (or linearized) damping coefficient and W is the weight displacement of a ship,.

The variation of GM with time is the key feature to model parametric roll. In the case of regular waves, when the variation of metacentric height is not very large, the dependence of GM on time can be approximated by a sinusoidal function:

$$GM(t) = GM_m + GM_a \cos(\omega_e t),$$

where GM_m is the mean value of the *GM*, GM_a is the amplitude of the *GM* changes in waves and ω_e is the wave frequency of encounter.

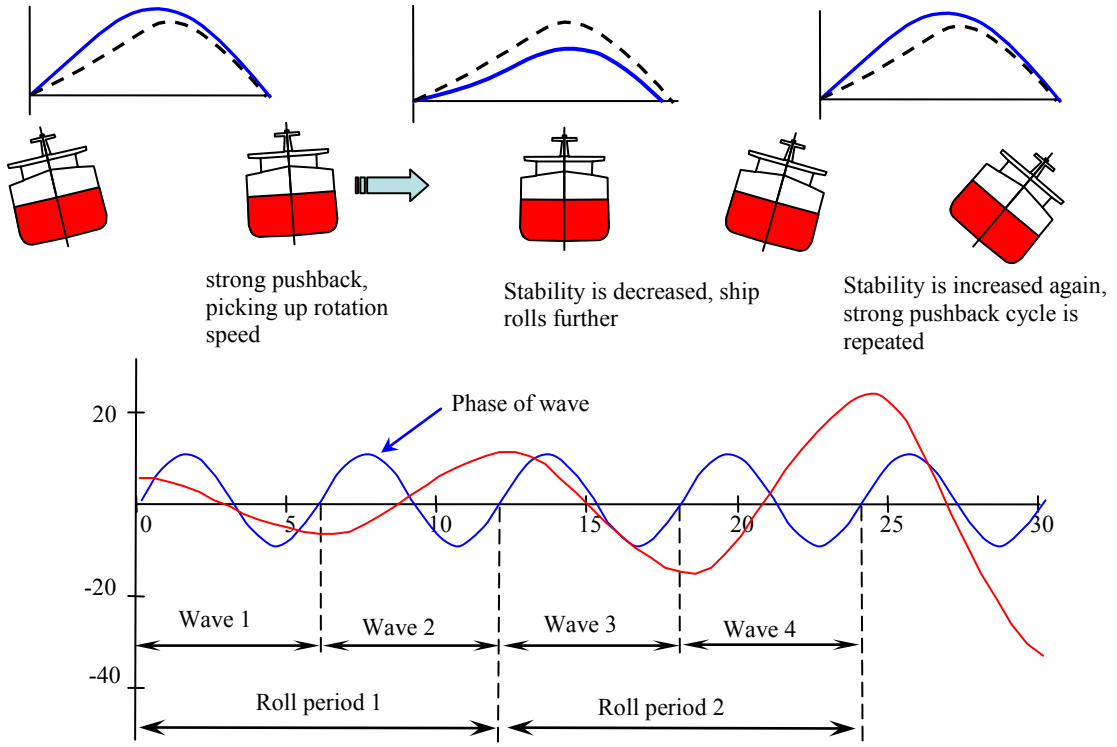

Figure 8. Development of Parametric Roll

As a first approximation, GM_m and GM_a can be determined as:

$$GM_a = 0.5\left(GM_{\max} - GM_{\min}\right), \tag{9}$$

and

$$GM_m = 0.5\left(GM_{\max} + GM_{\min}\right),$$

where $GM_{\max}$ and $GM_{\min}$ are the maximum and minimum values of the GM value for one passage of the wave crest along the ship hull. Alternatively, the actual average of GM in waves also can be used.

The Mathieu equation is derived by transforming Equation (8) into the canonical form:

$$\ddot{\phi} + 2\delta\dot{\phi} + \omega_m^2\left(1 + h\cos(\omega_e t)\right)\phi = 0, \tag{10}$$

where:

$$\omega_m = \sqrt{\frac{W \cdot GM_m}{I_x + A_{44}}}; \omega_a = \sqrt{\frac{W \cdot GM_a}{I_x + A_{44}}};$$

$$\delta = \frac{1}{2}\frac{B_{44}}{I_x + A_{44}}; h = \frac{\omega_a^2}{\omega_m^2}.$$

Then dimensionless time is introduced:

$$\tau = \omega_e t$$

this change of variable allows damping to be removed:

$$\phi(\tau) = x(\tau) \cdot \exp\left(-\mu\tau\right); \tag{11}$$

which finally leads to the Mathieu equation

$$\frac{d^2x}{d\tau^2} + \left(p + q\cos(\tau)\right)x = 0, \tag{12}$$

where:

$$p = \left(\overline{\omega}_m^2 - \mu^2\right); q = \overline{\omega}_m^2 h;$$

$$\mu = \frac{\delta}{\omega_e}; \overline{\omega}_m = \frac{\omega_m}{\omega_e}.$$

The solution of the Mathieu equation (12) cannot be expressed in elementary functions. A special function, the Mathieu function, has been introduced to describe the solution of equation (12). The most important characteristic of this solution is whether it is bounded or not (see Figure 9).

As shown in Figure 9, different combinations of the characteristics of coefficients p and q lead to either a bounded or unbounded solution. The Ince-Srutt diagram, shown in Figure 10, maps the bounded and unbounded solutions, depending on the coefficients, p and q. The shaded areas, identified with Roman numerals in Figure 10, correspond to the unbounded solution.

The first instability zone intersects the axis at exactly $p = 0.25$, which corresponds to the frequency ratio of 2; so the excitation frequency is twice the natural roll frequency at this point. The unbounded motion belonging to this zone is commonly referred to as the principal parametric resonance. The zoomed-in view of this zone is shown in the insert of Figure 10.

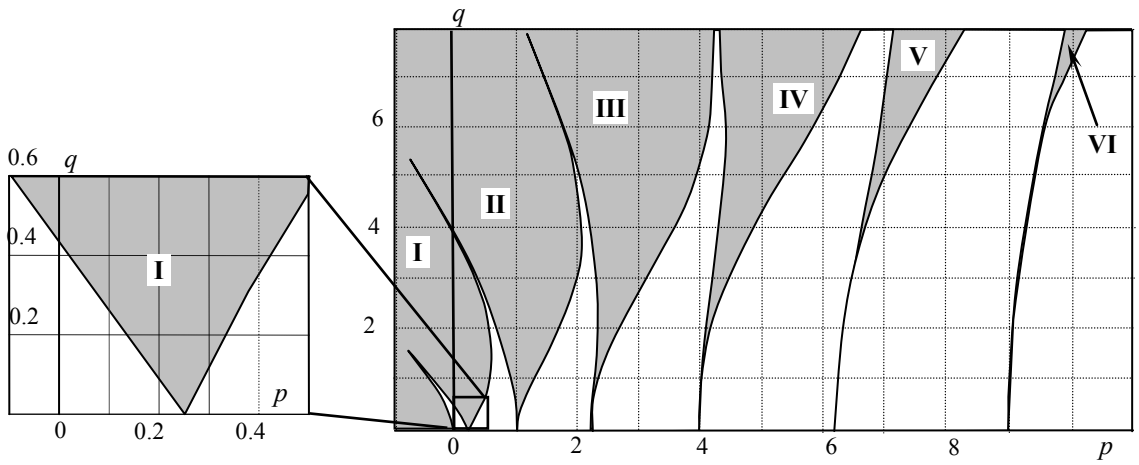

Figure 10 Ince-Strutt Diagram

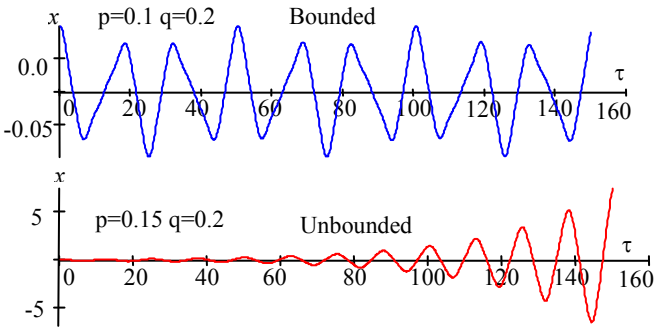

Figure 9: Bounded and Unbounded Solution of Mathieu Equation

The Mathieu equation (12) has a periodic-bounded solution since damping was excluded by the substitution (11). It means that the corresponding roll, $\phi(\tau)$, decays with the damping decrement, μ, if $x(\tau)$ is a periodical solution of the Mathieu equation, as shown in Figure 9. It also means that there is a threshold value for roll damping for each pair of Mathieu parameters, p and q. If roll damping is less than the threshold value, the roll will be unbounded as a solution of the Mathieu equation. If the roll damping is larger than the threshold, roll is bounded, even if the solution of the Mathieu equation is unbounded. The increment of the Mathieu solution is not enough to overcome the decrement of roll damping. It also means that with linear damping, the instability zone is narrower and requires some finite value of *GM* variations even at $p = 1/4$; *i.e.*, it does not touch the axis (see Figure 11).

The boundaries in indicating where parametric resonance is possible, reveal two interdependent conditions that may be used to formulate the following criteria: the frequency condition and the parametric excitation condition. The frequency condition depends on natural and encounter frequencies. Natural frequency depends on the loading condition, while encounter frequency depends on the wave parameters and the ship's speed and heading. The parametric-excitation condition requires that the change of stability is large enough to cause instability; whether this condition is satisfied depends on the hull geometry and on the parameters of the wave used for the assessment.

To derive a criterion for the critical parametric excitation that creates roll growth, consider an approximate solution of the Mathieu equation (10) for exact principal resonance ($\omega_e = 2\omega_m$), as presented by Hayashi (1985) and used to derive a "transient stage" criterion for parametric roll by Spyrou (2005) as follows:

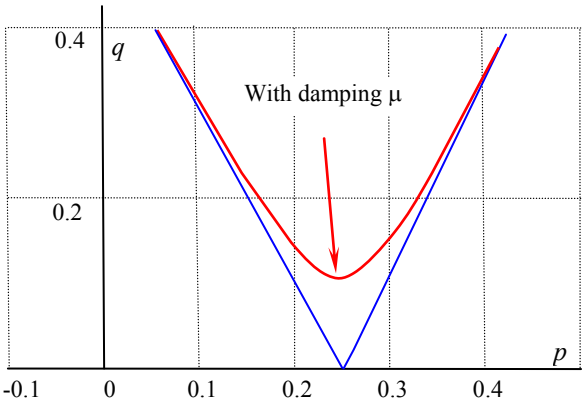

Figure 11. Influence of Damping on the 1st Instability Zone

$$\phi(t) = e^{-\delta t}\left[C_1 e^{\kappa\omega_m t}\sin(\omega_m t - \varepsilon) + C_2 e^{-\kappa\omega_m t}\sin(\omega_m t + \varepsilon)\right], \quad (13)$$

where C_1 and C_2 are arbitrary constants which are determined by the initial conditions and κ is a parameter controlling the growth or decay of oscillations. It is defined as:

$$\kappa = -\frac{1}{4}\sqrt{a^2h^2 - 4(a-1)^2},$$

where a is variable expressing the frequency ratio,

$$a = 4\frac{\omega_m^2}{\omega_e^2}.$$

Obviously, $a = 1$ when $\omega_e = 2\,\omega_m$, which is exactly the middle of the first instability zone (principal parametric resonance) of the Ince-Strutt diagram.

The phase ε is determined from the following expression,

$$\cos(2\varepsilon) = \frac{2(a-1)}{a\cdot h}; -\frac{\pi}{2} \le \varepsilon \le 0.$$

The encounter frequency of "dangerous" waves is considered to correspond exactly to the frequency of principal parametric resonance:

$$a = 1; \kappa = -\frac{h}{4}; \varepsilon = -\frac{\pi}{4}. \quad (14)$$

Looking at the initial condition when the initial roll rate has zero value, the constants are found equal to:

$$C_1 = -C_2 = \frac{\sqrt{2}}{2}\phi_0; \dot{\phi}_0 = 0. \quad (15)$$

Substituting Equations (14) and (15) into Equation (13) yields:

$$\phi(t) = \frac{\sqrt{2}}{2}\phi_0 e^{-\delta t}\left[e^{-\frac{h}{4}\omega_m t}\sin\left(\omega_m t + \frac{\pi}{4}\right) - e^{\frac{h}{4}\omega_m t}\sin\left(\omega_m t - \frac{\pi}{4}\right)\right] \quad (16)$$

Equation (16) allows calculation of the amplification factor, f, after n oscillations:

$$f = \frac{1}{\phi_0}\phi\left(\frac{2\pi n}{\omega_m}\right). \quad (17)$$

Note that the term with the negative exponent in Equation (16), plays a small role for a motion that is in fact growing exponentially. In this case, the substitution of Equation (16) into Equation (17) yields:

$$f = -\frac{\sqrt{2}}{2}\exp\left(\frac{\pi n h}{2} - \frac{2\delta\pi n}{\omega_m}\right)\sin\left(2\pi n - \frac{\pi}{4}\right). \quad (18)$$

Solving for h from Equation (18) leads to:

$$h = 2\frac{\ln f + \ln 2}{\pi n} + \frac{4\delta}{\omega_m}.$$

Given an amplification factor and the number of oscillations, the following criterion is deduced, assuming the stability changes in waves are symmetric relative to the calm water values:

$$\frac{GM_a}{GM_0} \ge 2\frac{\ln f + \ln 2}{\pi n} + \frac{4\delta}{\omega_0}. \quad (19)$$

The parameters δ and ω_0 in Equation (19) have to be chosen. If no other data are available, ABS (2004) recommends, as a conservative estimate,

$$\frac{\delta}{\omega_0} = 0.03. \quad (20)$$

The number of cycles and the amplification factor are obviously related. Larger amplification of the initial roll may be expected for more cycles. These parameters are very important for fine tuning the criteria and need to be addressed during a later stage of criterion development. As a preliminary guess of $f = 5$ and $n = 4$ leads to,

$$\frac{GM_a}{GM_0} \ge 0.5. \quad (21)$$

Equation (19) can also be used to derive a criterion without transient effects. Such a criterion identifies the existence of an unbounded solution, as the solution tends to go to infinity with an increase in the number of cycles,

$$\lim_{\substack{n\to\infty \\ f\to\infty}}\left(2\frac{\ln f + \ln 2}{\pi n} + \frac{4\delta}{\omega_0}\right) = \frac{4\delta}{\omega_0} \Rightarrow \frac{GM_a}{GM_0} \ge \frac{4\delta}{\omega_0}. \quad (22)$$

Using a conservative assumption on roll damping in Equation (20) leads to

$$\frac{GM_a}{GM_0} \ge 0.12. \quad (23)$$

As can be expected the exclusion of transient effects leads to a far more conservative standard. The importance of Equation (23) is that it sets a practical limit for the "conservativeness" of the standard, as the damping assumption in Equation (20) is extremely conservative. Another important point is that including transient effects in the criteria is similar to assuming less conservative damping. This effect is presented in detail in Appendix 1.

These criteria require knowledge of the magnitude of parametric excitation in Equation (9), which is based on calculations of the instantaneous GM in waves. While these calculations are straight forward, they involve computer software and additional time needed for preparation of geometric input. As was discussed above, most of the changes of the waterline for ships come from the bow and stern quarters of the hull, and these changes may be revealed by just altering the draft. Altering the draft was used for the Level 1 Vulnerability Criterion for pure loss of stability (2) proposed in SLF53/INF.10-Annex 2:

$$GM_a = \frac{I_{up} - I_{low}}{2V}, \quad (24)$$

where I_{up} and I_{low} indicate the moments of inertia of the water plane for upper and lower drafts, respectively, and V is the

displaced volume of the ship for a standard draft. It may be assumed the upper draft is lower than the freeboard's deck by 5% of freeboard, and the lower draft is half the mean draft or the intersection between the bilge circle and the side hull wall midship. Other proposals for these reference drafts can be found in SLF 53/3/9.

An obvious advantage of the criterion expressed in Equations (21) and (24) is its simplicity. The criterion can be evaluated without extra calculations, as all the values can be directly obtained from the vessel's hydrostatic curves. At the same time this criterion accounts for neither the ship's forward speed nor the likelihood of encountering dangerous environmental conditions. These factors may be determined by using the frequency of encounter for condition of parametric roll and by specifying the waves for the reference calculation.

The frequency of encounter can be determined using the boundaries of the first instability zone of the Ince-Strutt diagram. Because oscillations grow inside the instability zone and decay outside the instability zone, the solution has to be periodic at the boundary. To account for the damping already included in Equation(13), it is enough to satisfy:

$$\delta = \frac{h}{4}\omega_m,$$

to obtain the well-known approximation for the boundary of the first instability zone of Ince-Strutt diagram:

$$h = 2\sqrt{\left(1-\frac{1}{4}\frac{\omega_e^2}{\omega_m^2}\right)^2+\left(\frac{\omega_e\delta}{\omega_m^2}\right)^2}. \qquad (25)$$

This approximation establishes the relationship between coefficient q that is related to the magnitude of parametric excitation (9) and coefficient p, the ratio of the natural frequency to the frequency of encounter,

$$\omega_e = \omega - \frac{\omega^2}{g}V_m\cos\beta = \frac{\sqrt{2\pi}}{\lambda}\left(\sqrt{\lambda g} - V_m\sqrt{2\pi}\cos\beta\right)$$

where V_m is the forward speed in m/s, β is heading angle relative to the waves (0 is following seas), g is the acceleration due to gravity, ω is the true frequency of the wave, and λ is the wave length. Since the frequency of encounter depends on speed, Equation (25) can be used to determine whether if the design speed of a ship falls into a frequency range where parametric roll is possible,

$$V_{m1,m2} = \frac{\sqrt{g\lambda}}{\sqrt{2\pi}} - \frac{\lambda\sqrt{2(2\pm h)}}{T_\varphi}, \qquad (26)$$

where T_ϕ is the roll period.

A more sophisticated criterion can be proposed if actual wave parameters are taken into account. To account for the likelihood of encountering different waves, a series of wave cases could be used as proposed in Annex 1 SLF 53/INF.10 (see also Bulian & Francescutto, 2010). The final form of the criterion is similar to:

$$C_{PR1} = \sum_i W_i C(H_i,\lambda_i). \qquad (27)$$

Each wave case is defined by wave height H_i, and length, λ_i and W_i is the statistical weight of a given wave case. For each wave case the criterion is

$$C_i = \begin{cases} 1, & \text{if} \quad \dfrac{GM_a(H_i,\lambda_i)}{GM_m(H_i,\lambda_i)} \ge r \quad \text{and} \quad V_{PR} \le V_D, \\ 0, & \text{otherwise,} \end{cases} \qquad (28)$$

where

$$V_{PR} = \left|\frac{2\lambda}{T_\phi} - \sqrt{\frac{g\cdot\lambda}{2\pi}}\right|$$

and r is the ratio between the magnitude of GM changes and the mean value of magnitude providing the specified f-fold increase after n roll cycles, (preliminary value is 0.5); V_D is the design speed. V_{PR} is the speed where parametric roll is expected (wave encounter frequency is twice the roll natural frequency). Cases with negative GM_m require special handling.

The application of the criterion for parametric roll in Equation (27) obviously requires more computational work than evaluating Equation (21). However, these efforts may very well pay off if employing the application of Equation (27) indicates an absence of vulnerability to parametric roll, when the criterion in Equation (21) may be too conservative.

Sample calculations for the parametric roll Level 1 Vulnerability Criteria, are presented in Tables 3 and 4. Following the suggestion from SLF 53/3/7, the speed range criterion in Equation (26) was applied to the sample population of ships from SLF 53/INF.10 Annex 5, while a very conservative assumption was used for the magnitude of parametric excitation (h = 1) (see Table 3). As a result of using this conservative assumption, only the tanker was found not vulnerable.

The criterion and standard in Equation (21) were carried out using a wave with a length equal to ship length and with the steepness taken from SLF 53/3/7. The resolution of this criterion seems to be better, as it excluded bulk and LNG carries and both fishing vessels in addition to the tanker; these ships do not have known vulnerability to parametric roll (SLF 53/INF.10 Annex 5). Application of the approximation given in Equation (24) for the magnitude of the parametric excitation provides results that are similar in terms of resolution. Sample calculations for the criterion in Equation (28) are available from Bulian & Francescutto (2011).

Table 4 contains the results of calculations for the sample ship population from SLF 53/INF.10 Annex 10. The results in Table 4 (shown for two loading conditions) are qualitatively similar to those in SLF 53/INF.10 Annex 10. All the container carriers and the cruise vessel are found to be susceptible to parametric roll, while tugs, tankers and bulk carriers are not. Generally, this is consistent with existing operational experience. Multi-purpose vessels and the LNG carrier show vulnerability in certain loading conditions; thus their vulnerability must be determined by the level 2 criteria. Results for more loading cases are available for these ships in SLF 53/INF.10 Annex 10.

Level 2 Criteria for Parametric Roll

The linear equation of roll motion, Equation (8), as well as its particular case in Equation (10), is a good model to indicate the onset of parametric roll. However, it is not capable of estimating the amplitude of parametric roll; once parametric resonance in a linear system has started, its amplitude grows without any limit. Nonlinearity stabilizes parametric resonance at certain amplitude (see Figure 12).

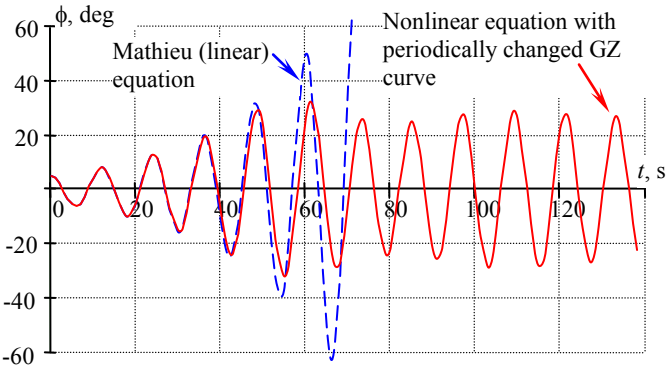

Figure 12. Modeling of Parametric Roll with Mathieu Equation (Dash) and Nonlinear Equation (Solid)

The mechanism of stabilization is related mostly to the nonlinearity of the GZ curve. Once the amplitude of the roll oscillation becomes large enough, the frequency condition for parametric resonance is no longer satisfied, as the change in instantaneous GM leads to a change in the instantaneous natural frequency. (It is a well-known phenomenon of nonlinear roll—the dependence of natural frequency on amplitude is also known as the loss of isochronous properties.) This means that once a certain roll amplitude has been exceeded, further flow of energy into the dynamical system stops. Additional energy is available only below this amplitude, which leads to the establishment of the energy/work balance and stabilization of the amplitude, and eventually leads to a limit cycle. Therefore, the simplest mathematical model capable of reproducing stabilization of parametric roll must include the nonlinear GZ curve:

$$(I_x + A_{44})\ddot{\phi} + B_{44}\dot{\phi} + W \cdot GZ(\phi, t) = 0$$

where $GZ(\phi,t)$ means a full GZ curve changing while the wave passes (see Figure 3).

Table 3 Sample Calculations on Parametric Roll, Level 1, based on Ships from SLF 53/INF.10 Annex 5

Ship	L, m	GM, m	V_s, kn	Criterion (26), h=1			Criterion and Standard (21)			
							GM in waves		Eq (24)	
				V_{s1}, kn	V_{s2}, kn	Y/N	Value	Y/N	Value	Y/N
Bulk Carrier	275	3.46	15	2.90	-24.48	Y	0.09	N	0.36	N
Bulk Carrier 2	145	0.56	15	12.96	1.02	Y	0.40	N	1.43	Y
Containership 1	322.6	1.27	25	16.22	-3.85	Y	1.42	Y	4.56	Y
Containership 2	376	1.79	25	17.05	-4.95	Y	0.90	Y	4.44	Y
Containership 3	330	1.85	25	10.31	-14.45	Y	0.58	Y	2.40	Y
Containership 4	283.2	1.15	25	8.43	-15.33	Y	0.75	Y	2.60	Y
Containership 5	262	2.00	25	7.45	-15.89	Y	0.77	Y	3.32	Y
Fishing Vessel 1	34.5	1.70	18	-6.08	-20.98	Y	0.16	N	0.47	N
Fishing Vessel 2	21.56	0.80	15	1.74	-5.24	Y	0.09	N	0.77	Y
General Cargo 1	121.9	0.67	18	14.40	5.29	Y	1.03	Y	1.03	Y
General Cargo 2	161.2	0.90	16	7.85	-8.99	Y	0.57	Y	1.54	Y
LNG Carrier	267.8	3.42	18	-1.16	-31.11	Y	0.18	N	0.62	Y
Naval Combatant 1	150	1.04	30	1.73	-18.79	Y	0.58	Y	5.25	Y
Naval Combatant 2	150	2.06	30	-18.0	-52.94	Y	0.60	Y	0.89	Y
Passenger Ship	276.4	3.75	25	-16.75	-58.59	Y	0.57	Y	0.97	Y
RoPax	137	1.79	18	-2.65	-25.41	Y	0.82	Y	1.40	Y
Tanker	320	9.95	14	-16.36	-60.16	N	0.03	N	0.21	N

Table 4 Sample Calculations on Parametric Roll, Level 1, based on Ships from SLF 53/INF.10 Annex 10

Ship	Description	*L*, m	*d*, m	GM1	Eq (24)	Y/N	GM2	Eq (24)	Y/N
Bulk Carrier	5500 DWT	190	12.8	2.84	0.2	N	3.34	0.17	N
Bulk Carrier		180	0.75	2.10	0.33	N	2.60	0.26	N
Containership	> 10000 TEU	360	16.0	0.80	3.76	Y	1.30	2.31	Y
Containership	> 10000 TEU	360	15.5	0.70	3.87	Y	1.20	2.26	Y
Containership	> 6000 TEU	320	14.6	0.70	4.28	Y	1.20	2.5	Y
Containership	> 6000 TEU	320	14.5	0.8	3.18	Y	1.30	1.96	Y
Containership	> 4000 TEU	250	13.5	0.50	3.03	Y	1.00	1.52	Y
Containership	> 4000 TEU	250	12.5	0.60	2.96	Y	1.10	1.62	Y
Containership	> 1000 TEU	210	12.0	0.60	2.71	Y	1.10	1.48	Y
Containership	> 1000 TEU	200	11.4	0.60	3.19	Y	1.10	1.74	Y
Containership	> 1000 TEU	170	10.9	0.50	3.6	Y	1.00	1.8	Y
Containership	> 1000 TEU	160	10.5	0.16	7.88	Y	0.66	1.91	Y
Containership	> 500 TEU	135	7.75	0.58	1.77	Y	1.08	0.95	Y
Containership	> 500 TEU	125	7.40	0.70	1.96	Y	1.20	1.14	Y
Cruise Vessel		240	7.20	2.71	0.86	Y	3.21	0.73	Y
LNG Carrier	1000 cbm	110	8.48	1.06	0.69	Y	1.56	0.47	N
MPV		135	8.00	0.65	0.91	Y	1.15	0.51	Y
MPV		125	7.00	0.17	3.23	Y	0.67	0.82	Y
MPV		120	7.08	1.00	0.98	Y	1.50	0.65	Y
MPV	7500 DWT	105	7.06	0.7	0.64	Y	1.20	0.37	N
Tanker	30000 DWT	320	22.6	6.35	0.08	N	6.85	0.08	N
Tanker		110	7.41	1.31	0.32	N	1.81	0.23	N
Tug		30	3.50	2.23	0.4	N	2.73	0.33	N
Tug		25	2.43	3.6	0.2	N	4.10	0.18	N

Nonlinear roll damping can also be a factor of stabilization. Its mechanism is slightly different from one with the GZ curve. An increase in the amplitude of roll motions leads to an increase in the roll rate magnitude when the ship crosses the equilibrium point. The increase in roll rate makes nonlinear damping large enough to elevate the threshold above the current level of parametric excitation. This also stops the flow of energy to the dynamical system and stabilizes the parametric roll.

However, roll-damping nonlinearity is relatively weak compared to GZ curve effects and should be considered as a secondary factor for stabilization in regular waves. (In irregular waves, the contribution from nonlinear roll damping may be different.) Also, if the roll amplitude is large enough, damping becomes dependent on the roll angle. This dependence may lead to a decrease of damping (when a bilge keel emerges from the water), as well as to an increase in damping (when the deck edge submerges into the water). Hence, this is dependent on ship-specific geometry (Bassler, *et al*., 2011). These considerations, however, make the mathematical model too complex for the second level vulnerability check, so it makes sense to limit the description of damping to a cubic or quadratic approximation:

$$\ddot{\phi} + f_d(\dot{\phi}) + \omega_\phi^2 \cdot f(\phi, t) = 0, \qquad (29)$$

where

$$f_d(\dot{\phi}) = 2\delta\dot{\phi} + \mathrm{sign}(\dot{\phi})\delta_2\dot{\phi}^2$$

or

$$f_d(\dot{\phi}) = 2\delta\dot{\phi} + \delta_3\dot{\phi}^3,$$

δ, δ_2 and δ_3 are the linear, quadratic and cubic damping coefficients, respectively; and $f(\phi,t)$ is a time-dependent stiffness term related to the instantaneous *GZ* curve in waves. The

damping coefficients can be found either from a roll decay test or by methods like Ikeda's semi-empirical formula.

As mentioned above, the calculation of the instantaneous GZ curve in regular waves is straightforward. However, the assumption of low-encounter frequency is not always applicable for parametric roll as it was for pure loss of stability, since the former may occur in head and bow-quartering seas as well as in following and stern-quartering seas.

The attitude of a ship is calculated based on the heave and pitch response to a regular wave:

$$\begin{cases} (M + A_{33})\ddot{\zeta}_G + B_{33}\dot{\zeta}_G + A_{35}\ddot{\theta} + B_{35}\dot{\theta} \\ \qquad + F_\zeta(\zeta_G, \theta, t) = F_H(t) \\ (I_Y + A_{55})\ddot{\theta} + B_{55}\dot{\theta} + A_{53}\ddot{\zeta}_G + B_{53}\dot{\zeta}_G \\ \qquad + M_\theta(\zeta_G, \theta, t) = M_H(t), \end{cases} \tag{30}$$

where M is mass of the ship; I_Y is the mass moment of inertia relative to the transverse axes; A_{33} and A_{55} are heave-added mass and pitch moment of inertia (assumed to be equal to the corresponding mass and moment of inertia), respectively; and B_{33} and B_{55} are damping coefficients for heave and pitch. F_H and M_H are hydrodynamic components of the wave excitation. Functions F_ζ and M_θ are the difference between hydrostatic and Froude-Krylov forces and moments, respectively, at the instant of time, t. These values are expressed as follows:

$$F_\zeta(\zeta_G, \theta, t) = \rho g \left(V_0 - \int_{-0.5L}^{0.5L} \Omega(x, z(\zeta_G, \theta, t))dx \right)$$

and

$$M_\theta(\zeta_G, \theta, t) = \rho g \left(V_0 \cdot LCB_0 - \int_{-0.5L}^{0.5L} M_\Omega(x, z(\zeta_G, \theta, t))dx \right)$$

where ρ is mass density of water, V_0 is volumetric displacement in calm water, and LCB_0 is the longitudinal position of the center of buoyancy in calm water. Functions Ω and M_Ω calculate an area and a static moment relative to the y-axis of a station located at a longitudinal position along the hull, x. The second argument of this function shows the submergence of this position along the hull, as expressed by the function of the instantaneous waterline $z(\zeta_G,\theta,t)$ (see Figure 13)

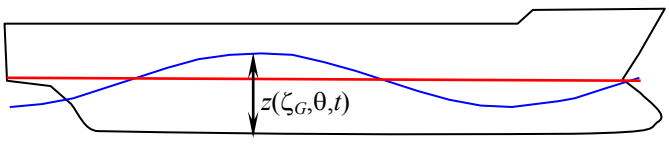

Figure 13 Sample Instantaneous Waterlines Evaluated from Heave and Pitch Response

Once the Froude-Krylov terms are defined, the system of differential Equations (30) can be integrated with a standard Runge-Kutta solver. Once the steady state of the response is reached, the instantaneous attitude of the ship for each position of the wave crest along the hull can be determined.

While this method for evaluating the heave and pitch attitude for stability in waves seems to be the most physically sound, several assumptions must be made regarding the heave and pitch hydrodynamic coefficients. If a seakeeping analysis has been performed at this stage in the design process, the added mass and damping are already available. If the vulnerability to parametric roll needs to be addressed earlier in the design process, additional assumptions are inevitable. The heave added mass and pitch added moment of inertia can be assumed equal to the corresponding mass and moment of inertia of the vessel. Simple assumptions (subject to further verification) can also be made for heave and pitch damping, based on typical values as a percentage of critical damping (40–50%). Finally, the diffraction excitation and hydrodynamic coupling coefficients can be neglected at this stage. It is quite simple to test these assumptions by direct comparison between the results of the simplified calculations and complete potential flow solutions. Such testing remains on agenda for the future work.

Once the attitude of the ship for each wave crest position has been determined, the GZ curve in waves can be evaluated. To calculate the GZ curve in waves, the current attitude of the vessel on the wave is considered to be in equilibrium following the d'Alembert's Principle, where the dynamical problem can be considered as a static problem if the inertial forces are added. These inertial forces show themselves as the difference between the current attitude and the equilibrium attitude on the wave for the same position of the wave crest. Further calculations of the GZ curve in waves are done in a usual way, utilizing the balancing of trim and draft at each heel angle. Models accounting for dynamic heave have also been developed and used by Kroeger (1986), Jensen (2007), and others.

Once the GZ curve in waves is available, roll Equation (29) is solved. It is a nonlinear ordinary, differential equation and does not have a known exact solution, leaving two options: an approximate analytical or a direct numerical solution. Both options allow consideration of nonlinear damping along with nonlinear restoring.

Approximate analytical methods for solution of the roll equation have been used extensively in the past (*e.g.* Sanchez & Nayfeh, 1990; Oh, *et al.,* 2000; Bulian, 2004; Spyrou, 2005) and have proven themselves to be quite efficient for relatively simple models. For example, the restoring function is considered in the following form:

$$f(\phi, t) = \phi + l_3\phi^3 + l_5\phi^5 + \frac{1}{GM}(GM_m - GM + GM_a \cos\omega_e t)\phi\left(1 - \left(\frac{\phi}{\pi}\right)^2\right),$$

where l_3 and l_5 are polynomial coefficients for the GZ curve in calm water. An approximate solution based on the first harmonic can be found using a well-known method such as "averaging" or "harmonic balance", as shown by:

$$\phi = \phi_a \cos(\omega t - \varepsilon), \omega = \omega_e / 2.$$

Then, the following algebraic equation can be obtained for deriving the steady-state amplitude, ϕ_a, of the periodic solution.

$$\pi^4\omega^2\left(\frac{3\phi_a^2\omega^2\delta_3+8\delta}{2\pi^2-\phi_a^2}\right)^2 + \frac{1}{16}\left(\frac{6\phi_a^2\omega_\phi^2-8\pi^2\omega_\phi^2}{\pi^2-\phi_a^2}\frac{(GM_m-GM)}{GM} - \pi^2\frac{5\phi_a^4 l_5\omega_\phi^2+6\phi_a^2 l_3\omega_\phi^2+8\left(\omega_\phi^2-\omega^2\right)}{\pi^2-\phi_a^2}\right)^2 = \omega_\phi^4\left(\frac{GM_a}{GM}\right)^2. \quad (31)$$

It can be shown that Equation (31) yields a linear solution if:

$$l_3 = l_5 = GM_m = 0; \omega = \omega_0. \quad (32)$$

Substitution of the above expressions in Equation (32) into Equation (31) reduces the latter to:

$$\frac{8\pi^2\delta_E}{(2\pi^2-\phi_a^2)\cdot\omega_0} = \frac{GM_a}{GM}, \quad (33)$$

where δ_E is the equivalent linear damping. Equation (33) is consistent with the level 1 criterion in Equation (22). This can be shown by letting the amplitude, ϕ_a, be small. Then, the equivalent linear damping, δ_E, becomes linear damping, δ, and with the square of the roll amplitude being small relative to $2\pi^2$, Equation (33) reduces to Equation (22).

Numerical solution of Equation (29) can directly utilize the results of the calculation of the GZ curve in waves. Another advantage of the numerical approach is the possibility of obtaining a transient solution, which avoids unnecessary conservatism in cases where parametric roll grows so slowly that the ship does not reach a large-roll angle in irregular seas (*cf.* Peters, *et al.*, 2010; also Annex 5 of SLF 53/INF.10). Application of a wave group, consisting of limited number of waves with the same length and height, leads to the same result as the "typical" wave group. Using such wave groups limits the calculation of stability in waves to only one type of wave. This significantly reduces the otherwise substantial number of calculations needed in the numerical approach (Annex 9 of SLF 53/INF.10).

Sample calculations using a direct numerical solution are shown in Tables 5 and 6. These calculations are based on the sample ship population from Annexes 5 and 10 of SLF 53/INF.10, respectively. These results are of a preliminary nature as the procedure for calculations has not yet been established. The initial heel angle used in

Table 5 was 10 degrees, while 5 degrees was used in Table 6. The initial roll rate was zero in both cases. Sample calculations using approximate analytical solution in Equation (31) can be found in Annex 2 of SLF 53/INF.10

Table 5 Sample Calculations on Parametric Roll, Level 2, based on Ships from SLF 53/INF.10 Annex 5

Ship	Description	L, m	GM, m	δ/ω□	Roll	Y/N
Bulk Carrier		275	9.4	0.05	10	N
Bulk Carrier 2		145	0.53	0.05	10	N
Containership 1	Post-panamax	322.6	1.11	0.05	>25	Y
Containership 2	Post-panamax	376	1.84	0.05	>25	Y
Containership 3	Post-panamax	330	1.64	0.05	>25	Y
Containership 4	Panamax	283.2	1.06	0.05	>25	Y
Containership 5	C11 Class	262	1.91	0.05	>25	Y
Fishing Vessel 1	Japanese Purse Seiner	34.5	1.69	0.05	10	N
Fishing Vessel 2		21.56	0.73	0.05	10	N
General Cargo 1	Series 60 C_B = 0.7	121.9	0.24	0.05	10	N
General Cargo 2	C4 Class	161.2	1.10	0.05	14.9	N
LNG Carrier		267.8	3.40	0.05	10	N
Naval Combatant 1	ONR Tumblehome	150	1.03	0.15	10	N
Naval Combatant 2	ONR Flared	150	3.01	0.15	10	N
Passenger Ship		276.4	3.70	0.05	>25	Y
RoPax		137	1.77	0.05	>25	Y
Tanker		320	9.76	0.05	10	10

Table 6 Sample Calculations on Parametric Roll, Level 2, based on Ships from SLF 53/INF.10 Annex 10

Ship	Description	*L*, m	*d*, m	GM1	Roll	Y/N	GM2	Roll	Y/N
Bulk Carrier	5500 DWT	190	12.8	2.84	5	N	3.34	5	N
Bulk Carrier		180	0.75	2.10	5	N	2.60	5	N
Containership	> 10000 TEU	360	16.0	0.80	32	Y	1.30	32	Y
Containership	> 10000 TEU	360	15.5	0.70	>35	Y	1.20	>35	Y
Containership	> 6000 TEU	320	14.6	0.70	32	Y	1.20	32	Y
Containership	> 6000 TEU	320	14.5	0.8	32	Y	1.30	32	Y
Containership	> 4000 TEU	250	13.5	0.50	31	Y	1.00	31	Y
Containership	> 4000 TEU	250	12.5	0.60	32	Y	1.10	32	Y
Containership	> 1000 TEU	210	12.0	0.60	32	Y	1.10	31	Y
Containership	> 1000 TEU	200	11.4	0.60	32	Y	1.10	31	Y
Containership	> 1000 TEU	170	10.9	0.50	32	Y	1.00	32	Y
Containership	> 1000 TEU	160	10.5	0.16	32	Y	0.66	30	Y
Containership	> 500 TEU	135	7.75	0.58	32	Y	1.08	31	Y
Containership	> 500 TEU	125	7.40	0.70	31	Y	1.20	30	Y
Cruise Vessel		240	7.20	2.71	31	N	3.21	30	N
LNG Carrier	1000 cbm	110	8.48	1.06	10	Y	1.56	5	N
MPV		135	8.00	0.65	23	Y	1.15	9	N
MPV		125	7.00	0.17	30	Y	0.67	13	N
MPV		120	7.08	1.00	30	Y	1.50	22	Y
MPV	7500 DWT	105	7.06	0.7	16	N	1.20	7	N
Tanker	30000 DWT	320	22.6	6.35	5	N	6.85	5	N
Tanker		110	7.41	1.31	5	N	1.81	5	N

The main result of calculations is an observed maximum roll angle. In a case of no parametric resonance, roll motions will decay and the maximum roll angle will be the initial angle. This will be the case for tankers, bulk and gas carriers, and naval combatants. Quick development of parametric roll is observed for container carriers, RoPax and cruise vessels; and these results are consistent with existing experience.

General cargo and multi-purpose vessels as well as fishing vessels are in a "grey" area. While the two sample fishing vessels in the above table did not indicate any vulnerability to parametric roll, fishing vessels, in principle, are known to be susceptible to parametric roll (*e.g.* Neves, *et al.,* 2009). In principle, general cargo ships can exhibit parametric roll in following seas under the condition of insufficient stability (Paulling, *et al.,* 1972, 1974, 1975). Some differences in the severity of the parametric roll response were observed in case of MPVs, depending on their loading conditions (see Table 6).

The question remains about what roll angle should be used as a standard. The ABS Guide (2004) used 22.5 degrees; this value came from a limit on the main engine operability for container carriers. It is based on lubrication requirements at static inclinations. Another standard might be proposed based on container-lashing requirements; this seems to be logical, but it may not be an appropriate criteria basis for other types of vessels. While the issue of the allowable roll angle needs further discussion, 20 degrees was used here to indicate vulnerability to parametric resonance.

An important observation is that the result of sample calculations for level 2 vulnerability criteria is, in general, less conservative than the level 1 vulnerability criteria. The results are consistent because all of the ships found to be non-vulnerable by the level 1 criteria have been found non-vulnerable by the level 2 as well.

VULNERABILITY CRITERIA FOR SURF-RIDING AND BROACHING-TO

Physical Background of Surf-riding and Broaching-To

Broaching-to is a violent uncontrollable turn, which occurs despite maximum steering effort. As with any other sharp-turn event, broaching-to is accompanied with a large heel angle, which may lead to partial or total stability failure. Broaching-to is mostly associated with operating in following and stern-quartering seas. Stability failure caused by broaching-to is known as a problem mainly for fishing vessels and high-speed, monohull passenger ships.

Broaching-to is often preceded by surf-riding. Surf-riding occurs when a wave, approaching from the stern, "captures" a ship and accelerates the ship to the wave-phase speed (wave celerity). To the outside observer, surf-riding looks like a transition from periodic surging (when waves overtake a ship) to a situation where a ship runs with a wave.

This transition is a well-known and established nonlinear phenomenon that has been discussed several times in the literature (e.g. Grim, 1951; Kan, 1990). From a nonlinear dynamics perspective, the fundamental dynamic sequence that leads to surf-riding and then to broaching-to has been identified by Spyrou (1996, 1997). As this phenomenon is well understood, at least in a deterministic environment, it seems viable to develop meaningful and scientifically sound criteria expressing the likelihood of surf-riding.

As surf-riding is in most cases a stationary condition, the wave profile does not vary relative to the ship. Furthermore, during surf-riding some ships exhibit dynamic yaw instability, despite active control. This leads to the uncontrollable turn identified as broaching-to. Therefore, the likelihood of surf-riding could be used in order to formulate suitable vulnerability criteria for broaching-to. For surf-riding to occur, the wave length is usually comparable with the ship length. Large ships cannot surf-ride because waves of the necessary length are simply too fast compared to the ship speed.

Surf-riding is an equilibrium condition in which the sum of the wave-induced surge force, propeller thrust (at given speed settings) and resistance is zero, with the ship speed equal to the wave celerity. As can be seen from Figure 14, there are two crossings and, therefore, two equilibria on the span of one wave. One of these equilibria is located near the wave crest. It is unstable in surge in that if a ship is perturbed from this position, it will continue the motion rather than returning to the equilibrium position. The other equilibrium position located near the wave trough and is stable in surge, in that if a ship is perturbed from this position, it will return to the equilibrium position.

There are two characteristic speed settings or nominal Froude numbers, associated with surf-riding. One is called the critical speed for surf-riding under *certain* initial conditions (or the first critical speed, or the first threshold), and the other is critical speed for surf-riding under *any* initial conditions (Makov, 1969). The critical speed for surf-riding under certain initial conditions is where surf-riding equilibrium exists.

Surging motions, however, are still possible, even when surf-riding equilibria exist which is shown in the phase plane diagram (Figure 15). Some combinations of the ship's position on the wave and its instantaneous forward velocity correspond to surf-riding while others combinations correspond to surging.

The origin of the coordinate system in Figure 15 is located on a wave crest and therefore, it moves with the wave celerity. Surf-riding corresponds to the points on the *x*-axis relative to the position of the wave crest (at which the ship is moving at the wave celerity—ξ_G is zero). While the ship is surging, its mean speed is less than the wave celerity (i.e., ξ_G is negative), which means that the surging trajectories are shown as dashed lines leading backwards and away from the wave crest. The shaded area in Figure 15 shows combinations of a position on the wave and instantaneous forward speed relative to the wave celerity that lead to surf-riding; the rest of the phase plane corresponds to surging.

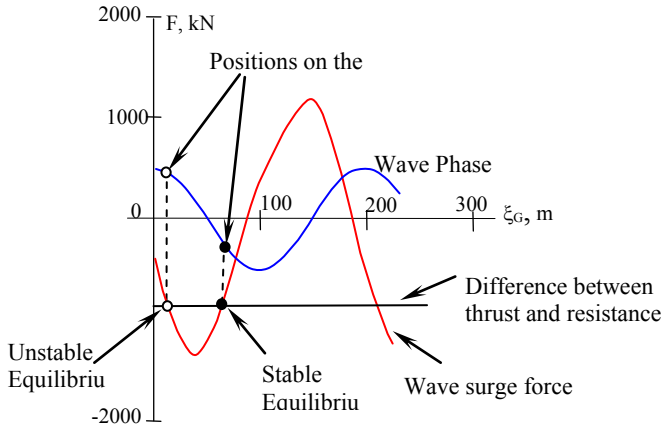

Figure 14. Surf-Riding Equilibria for a 100 m High-speed Vessel, Wave Height 6 m, Wave length 200 m, Speed Setting 24 kn

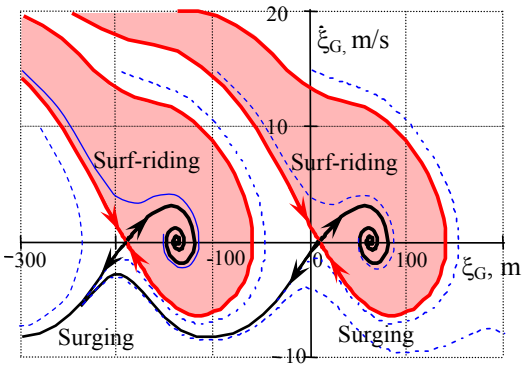

Figure15. Phase Plane with Surging and Surf-Riding (Belenky, *et al*., 2008)

Surging and surf-riding do not coexist for all speeds. Increasing the ship's speed causes the surf-riding area to grow, until the surging area ceases to exist (see Figure 16). The speed (or nominal Froude number) corresponding to that situation is regarded as the critical speed for surf-riding under any initial conditions, or the second critical speed (or the second threshold). If one considers the phase plane comprised by the pair of ship's longitudinal position and velocity, surf-riding will appear as occurring under any initial conditions (somewhere between 23.25 and 23.5 knots in Figure 16).

For a general discussion, these critical speeds (the first one appears when surf-riding becomes possible; and the second (higher) one, when surf-riding becomes inevitable) are more conveniently expressed in terms of the nominal Froude number

rather than as dimensional speeds. These two Froude numbers are the major characteristics of the likelihood of surf-riding. Wave capture associated with surf-riding is not just an acceleration phenomena, in fact if wave capture occurs while going faster that the wave celerity, deceleration will occur. However, this type of surf-riding is only relevant for very high-speed craft, so it is not discussed here.

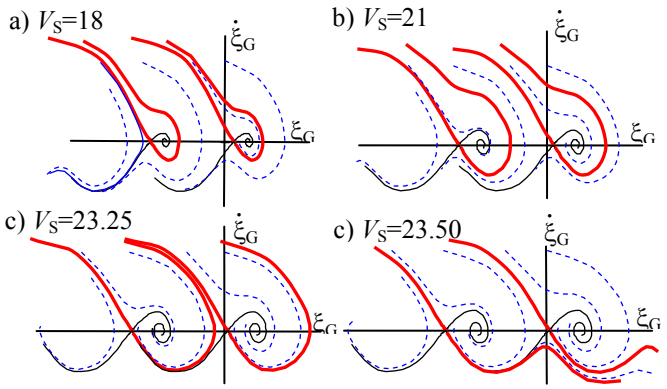

Figure 16 Changes of the Phase Plane with Increase of Speed Settings

Mathematical Model for Surf-riding

Because surf-riding is often a pre-requisite to broaching-to, the development of the vulnerability criteria focuses on surf-riding, as the mathematical modeling is simpler than for broaching-to.

Identification of the first critical speed is simple, as the calculation of the Froude-Krylov surge-wave force is straight forward. This force is a result of the integration of the incident wave pressure in the absence of the ship over the surface of the hull (a derivation is shown in Belenky & Sevastianov, 2007):

$$F_W(\xi_G) = -\rho g k \zeta_A [A_S \sin(k\xi_G) - A_C \cos(k\xi_G)] \qquad (34)$$

where

$$A_S = \int_{-0.5L}^{0.5L} A_0(x) \cdot \cos(kx) dx, \quad A_C = \int_{-0.5L}^{0.5L} A_0(x) \cdot \sin(kx) dx; \qquad (35)$$

$$A_0(x) = 2 \int_{d(x)}^{0} y(x,z) \exp(kz) dz, \qquad (36)$$

and x, y and z are the coordinates of points on the surface of the hull, expressed in a ship-fixed coordinate system; $y(x, z)$ is the half-breadth on a station with coordinate x at depth z; $d(x)$ is the draft of a station at longitudinal position x; k is the wave number; ζ_A is the wave amplitude; and ρ is the mass density of water.

The above prediction method shows reasonable agreement with model experiments except for ships with very fine forms where it is believed that nonlinear wave effects may be significant. While effects of nonlinear incident waves are rather limited, even in steeper waves; three-dimensional diffraction effects may be important for some ships (Sadat-Hosseini, *et al.*, 2011).

Once the amplitude for the wave-surging force is calculated, the first threshold can be found by solving the following algebraic equation relative to speed (thrust) setting, expressed as the commanded rps, n.

$$R(c) - T(c,n) + \rho g k \zeta_A \sqrt{A_S^2 + A_C^2} = 0, \qquad (37)$$

where R is the resistance in calm water, T is the, and c is the wave celerity.

While the calculation of the first threshold is simple, it may not be the most appropriate choice for setting a criterion because, when the equilibrium first appears, its domain of attraction is small (see Figure 16a). Also, the first threshold is higher than the surging trajectory for the nominal speed and, as a result, the ship is not likely to enter this domain without additional force being applied. Thus, a criterion derived from Equation (37) would unnecessarily penalize ships.

Calculation of the second threshold is more involved, as it requires examining the behavior of the boundary between the domains of surf-riding and surging. To understand this, the simplest mathematical model describing surf-riding and surging can be considered:

$$(m + m_x) \cdot \ddot{\xi}_G + R(c + \dot{\xi}_G) - T(c + \dot{\xi}_G, n) + F_W(\xi_G) = 0, \qquad (38)$$

where m is the mass of the ship, m_x is the surge added mass, ξ_G is the distance between the wave crest and the center of gravity of the vessel, c is the wave celerity, and n the commanded rps of the propeller (i.e., the speed or thrust setting) is an independent parameter.

Equation (38) can be solved numerically for a given pair of initial conditions: ship position on the wave and instantaneous speed (i.e., a single point in the phase plane). The equation needs to be solved only long enough to indicate whether the ship is surging or surf-riding. The initial conditions can be plotted on a graph: *e.g.* black for surf-riding; white for surging. Placing these initial conditions in the nodes of a grid, it is possible to find an approximate location of the boundary. The process must be repeated for different speed settings until all the initial conditions produce surf-riding. Since determining the threshold is the objective, the calculations can be limited to few indicative pairs of initial conditions with relatively low-initial instantaneous speed.

Another way to determine the threshold is by detecting the change of the shape of the boundary between the domains of surf-riding and surging. This approach requires determining the boundary; comprised of the unique trajectory, that leads towards unstable equilibrium. Positions of equilibria are found from Equation (38) by letting $\ddot{\xi}_G = \dot{\xi}_G = 0$,

$$R(c) - T(c,n) + F_W(\xi_G) = 0. \qquad (39)$$

If the speed settings are above the first threshold, Equation (39) must have two solutions (ξ_{GS}; ξ_{GU}), corresponding to stable and unstable equilibria, respectively (see also Figure 14). The boundary between surging and surf-riding can be found by integration starting from an unstable equilibrium. Since the

difference between the wave and ship speed at unstable equilibrium is zero, the initial conditions for integration need to be chosen, slightly shifted from unstable equilibrium, in the eigen-direction defined by the following equation that refers to the local-linearized system (see Figure 17):

$$\dot{x} = \left(-\delta_x - \sqrt{\delta_x^2 + k_{WL}} \right) x.$$

The coefficients δ_x and k_{WL} are determined by local linearization at the unstable equilibrium, ξ_{GU},

$$k_{WL} = -\frac{1}{(m+m_x)} \frac{dF_W(\xi_G)}{d\xi_G}\bigg|_{\xi_G = \xi_{GU}},$$

$$\delta_x = \frac{1}{2(m+m_x)} \frac{dR(\dot{\xi}_G)}{d\dot{\xi}_G}\bigg|_{\dot{\xi}_G = 0}.$$

The application of Newton's method allows the direct detection of this threshold (Umeda, *et al*., 2007).

An analytical, approximate but highly nonlinear method, the so-called Melnikov's method, can produce a practical criterion of surf-riding in closed form (Kan, 1990; Spyrou, 2006). The idea is based on the fact that the boundaries overlap when the ship speed (i.e., thrust) settings correspond to the second threshold. Melnikov's function reflects the distance in the phase plane between the two boundaries. Therefore, the instant of achieving the second threshold corresponds to the zero-value of Melnikov's function.

For a dynamical system, a closed-form expression of the Melnikov function is sometimes approximated as a perturbation from a Hamiltonian system. Practically, this means that the system should be relatively lightly damped, while a Hamiltonian system can include nonlinearity in the stiffness term. In contrast with other perturbation methods, Melnikov's method does not require small nonlinearity in the restoring term in order to be applicable. One can also relax the requirement of low damping, but this would be at the expense of not obtaining a closed form solution. To apply Melnikov's method, thrust and resistance are expressed with elementary functions and Equation (38) is transformed into the following non-dimensional form:

$$x'' + p_1(n)x' + p_2 x'^2 + p_3 x'^3 + \sin x = r(n),$$

where $x = k\xi_G$, with k the wave number; r the quasi-static part of the balance between thrust and resistance; coefficients, p_1, p_2, and p_3, represent the change of this balance; and n is the current speed (thrust) setting.

As shown in (Spyrou, 2006), Melnikov's function can be expressed as,

$$M(n) = -r(n) - \frac{4}{\pi} p_1(n) + 2p_2 - \frac{32}{3\pi} p_3. \qquad (40)$$

The speed setting corresponding to the "second" threshold n_{Tr2} can be identified from Equation (40), by satisfying the condition:

$$M(n_{tr2}) = 0.$$

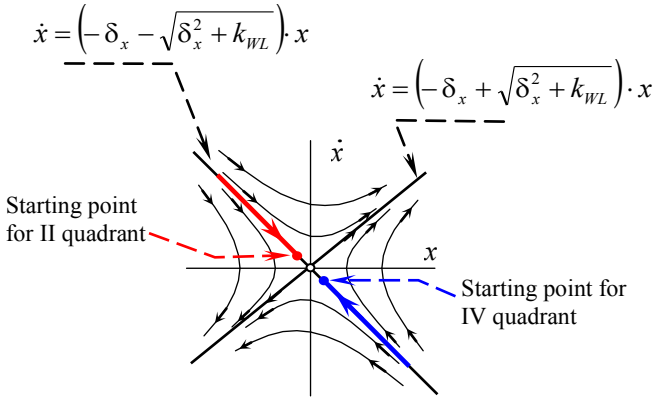

Figure 17. Initial Conditions for Calculation of the Boundary

Level 1 Vulnerability Criteria for Surf-riding and Broaching-to

The "second" surf-riding threshold is already used in MSC.1/Circ. 1228 as operational guidance for avoiding the danger of broaching. First introduced in 1995 by MSC.707, this threshold was based on phase-plane analyses of surging and surf-riding for a number of ships, using a wave steepness of 1/10. The analysis resulted in the following formula:

$$V_S \geq \frac{1.8\sqrt{L}}{\cos(180-\alpha)}, \text{ kn}, \qquad (41)$$

where L is length of the ship, α is wave heading (0° is head waves). Assuming following seas (α = 180°) and transforming Equation (41) into the form of length-based Froude number yields:

$$Fn \geq \frac{1.8 \cdot 0.51444}{\sqrt{g}} = 0.296 \approx 0.3 \qquad (42)$$

Taking advantage of the experience with the application of MSC.1/Circ. 1228, it makes sense to consider Equation (42) as a level 1 vulnerability criterion. Thus, ships with service speeds exceeding Fn = 0.3 should be subject to the level 2 vulnerability check. In general, this is supported by calculations of the second threshold using strip theory for surging force (Equations (34)–(36), with further direct analytical detection by the Melnikov method (Spyrou, 2006) or by numerical integration along invariant manifolds with Newton's method (Umeda, *et al.,* 2007). Umeda & Yamamura (2010) reported that the second threshold could be slightly below Fn = 0.3 for certain types of vessels, though further study by Umeda, *et al*. (2011) did not support this. One reason why calculations can sometimes show the second threshold below Fn = 0.3 is the overestimation of surging forces for some particularly fine ship forms.

Assuming the Froude number as a vulnerability criterion and 0.3 as a standard, it is necessary to recognize that this criterion's physical background is related to a wave steepness of 1/10. This wave steepness is quite high and the likelihood of encountering a long and steep wave is less than the likelihood of encountering a short and steep wave. Accepting Fn = 0.3 as an

"across-the-board" criterion and standard may unnecessarily penalize long ships, thus the length of a ship needs to be included in the criterion. Document SLF-53/3/8 considers vulnerability for surf-riding and broaching-to only for a ship when its length is less than 200 m.

The critical wave/wave group approach (Themelis & Spyrou, 2007) combines the probabilistic nature of realistic waves and a deterministic description of ship dynamics. Umeda & Yamamura (2010) examined estimates of the probability of broaching-to, using ships of different lengths. First, combinations of wave height and wave length leading to dangerous broaching-to were determined by numerical simulations in regular waves. Then, the probability of encountering these waves was evaluated using the Longuet-Higgins method (Longuet-Higgins, 1983). Finally, the probability of broaching-to was estimated as the probability of encountering a wave capable of causing broaching-to (Umeda, *et al*., 2007). The simultaneous increase of the wave length and wave height lead to a decrease of the probability of broaching-to. Similar conclusions were reached by Peters, *et al*. (2011).

Results from applying the proposed criteria to the sample ships are given in Tables 7 and 8. The service speed was assumed to be 1 knot below the design speed. Only two ships from Table 7 and four ships from Table 8 were shown to have vulnerability to surf-riding and broaching-to as their length is below 200 m and the Froude number, corresponding to service speed exceeded 0.3. The fishing vessels and naval combatants from Table 8 are generally known for their vulnerability to surf-riding. The tugs from Table 7 show vulnerability to surf-riding because they are short and powerful. However, because the operation of these relatively small tugs in open sea is unlikely, surf-riding and broaching-to is not a hazard for them.

Level 2 Vulnerability Criteria for Surf-riding and Broaching-to

Similar to pure loss of stability, the phenomenon of surf-riding is often a single-wave event. Despite the fact that the process of attraction to a surf-riding equilibrium takes some time, the disappearance of the equilibrium is instantaneous. The vulnerability to surf-riding can be measured by the percentage of waves capable of generating surf-riding. To do so, the irregular seaway is modeled as a sequence of sinusoidal waves with random lengths and amplitudes and the statistical weight of each wave is calculated using Equation (3). The results can be regarded as the probability of occurrence of surf-riding when a ship meets a wave with the assumed wave length and amplitude.

Direct calculation of the second threshold by Melnikov's method or a numerical method using the phase plane was considered too complex for the level 1 vulnerability criterion. However such level of complexity is consistent with requirements for level 2.

For each wave with a specific length and amplitude associated with a wave spectrum, the speed of the ship is compared with the speed corresponding to the "second" threshold for surf-riding, calculated by Melnikov's method. This comparison (using Froude number, *Fn*) yields a factor $C2_{ij}$:

$$C2_{ij} = \begin{cases} 1 & \text{if } Fn > Fn_{TR}(\lambda_i, a_j) \\ 0 & \text{if } Fn \le Fn_{TR}(\lambda_i, a_j). \end{cases}$$

The weighted average of the factor, $C2_{ij}$, which is determined over all of the values of λ_i and a_j, is the key element of the criterion:

$$C2(H_S, T_Z) = \sum_{i=1}^{N_\lambda} \sum_{j=1}^{N_a} W_{ij} C2_{ij}, \qquad (43)$$

Table 7. Sample Calculations for Surf-riding Level 1 Criteria, based on Ships from SLF 53/INF.10 Annex 10

Ship	Description	*L*, m	V, kn	Fn	Fn > 0.3 ?	Ship	Description	*L*, m	V, kn	Fn	Fn > 0.3 ?
Bulk Carrier	5500 DWT	190	14	0.15	N	Containership	>500 TEU	135	18	0.24	N
Bulk Carrier		180	14	0.16	N	Containership	>500 TEU	125	18	0.25	N
Containership	>10000 TEU	360	25	0.21	N	Cruise Vessel		240	22	0.22	N
Containership	>10000 TEU	360	24	0.20	N	LNG Carrier	1000 cbm	110	16	0.23	N
Containership	> 6000 TEU	320	25	0.22	N	MPV		135	15	0.20	N
Containership	> 6000 TEU	320	25	0.22	N	MPV		125	15	0.21	N
Containership	> 4000 TEU	250	24	0.24	N	MPV		120	17	0.24	N
Containership	> 4000 TEU	250	25	0.25	N	MPV	7500 DWT	105	13	0.19	N
Containership	> 1000 TEU	210	17	0.18	N	Tanker	30000 DWT	320	14	0.12	N
Containership	> 1000 TEU	200	22	0.24	N	Tanker		110	13	0.19	N
Containership	> 1000 TEU	170	20	0.24	N	Tug		30	12	0.33	Y
Containership	> 1000 TEU	160	20	0.25	N	Tug		25	11	0.33	Y

Table 8. Sample Calculations for Surf-riding Level 1 and 2 Criteria, based on Ships from SLF 53/INF.10 Annex 5

Ship	Description	*L*, m	V, kn	Fn	Fn > 0.3 ?	C2	$C2_L$	$C2_L$ > 0.01 ?
Bulk Carrier		275	16	0.15	N	0.00	0.00	N
Bulk Carrier 2		145	14	0.18	N	0.00	0.00	N
Containership 1	Post-panamax	323	25	0.22	N	0.00	0.00	N
Containership 2	Post-panamax	376	25	0.20	N	0.00	0.00	N
Containership 3	Post-panamax	330	25	0.22	N	0.00	0.00	N
Containership 4	Panamax	283	25	0.23	N	0.00	0.00	N
Containership 5	C11 Class	262	25	0.24	N	0.00	0.00	N
Fishing Vessel 1	Japanese Purse Seiner	35	17	0.44	Y	0.56	0.285	Y
Fishing Vessel 2		22	14	0.46	Y	0.34	0.175	Y
General Cargo 1	Series 60 C_B = 0.7	122	18	0.25	N	0.00	$3\ 10^{-9}$	N
General Cargo 2	C4 Class	161	18	0.22	N	0.00	0.00	N
LNG Carrier		268	18	0.17	N	0.00	0.00	N
Naval Combatant 1	ONR Tumblehome	150	30	0.39	Y	0.20	0.22	Y
Naval Combatant 2	ONR Flared	150	30	0.39	Y	0.20	0.22	Y
Passenger Ship		276	25	0.24	N	0.00	0.00	N
RoPax		137	19	0.25	N	0.00	$5\ 10^{-5}$	N
Tanker		320	14	0.12	N	0.00	0.00	N

where criterion *C*2, is a function of the significant wave height, H_S, and the mean zero-crossing period, T_Z, since the distribution of wave numbers and amplitudes used for calculation of statistical weights, depends on the spectrum defined using these parameters.

The long-term formulation of the criterion can be found by averaging Equation (43) over the values of significant wave heights and mean zero-crossing periods using entries of the wave scatter diagram as weights:

$$C2_L = \sum_{H_S} \sum_{T_Z} C2(H_S, T_Z) P(H_S, T_Z),$$

where $P(H_S,T_Z)$ is the statistical frequency of observation of a sea state with significant wave height, H_S, and mean zero-crossing period, T_Z. The data for averaging between different sea states can be obtained with the standard wave scatter diagram (*i.e.* IACS 2001):

$$P(H_S, T_Z) = \frac{N(H_S, T_Z)}{N_{Tot}},$$

where $N(H_S,T_Z)$ is the number of observations of a particular sea state and N_{Tot} is the total observations available.

Table 8 contains the results of calculations carried out on a sample population of ships. The value of criterion C2 was calculated for a single wave-state characterized with H_S = 2.5 m, T_Z = 8.5 s (short-term criterion). Assuming a standard of 0.01, the susceptibility to surf-riding and broaching-to is predicted for both fishing vessels and naval combatants. This prediction is generally consistent with operational experience. The differences between short-term and long-term criteria seem to be minimal. The long-term criteria seem to be more sensitive as it covers more wave-height/wave-length combinations. The results are also consistent with the level 1 vulnerability criterion.

DIRECT STABILITY ASSESSMENT AND FUTURE OUTLOOK

Tools

Once the vulnerability to a certain mode of stability failure has been established, a direct assessment of dynamic stability is expected to follow, as defined in the framework of the second generation intact stability criteria (Annex 2 SLF 51/4/1). The objective of the direct stability assessment is two-fold: one is as a tool for detailed design analysis and the other is as a tool for the development of ship-specific operational guidance. At the core of direct stability assessment lies a method capable of reproducing ship motions in severe seas, with sufficient fidelity for sound, technical decision-making.

Considering the current state-of-the art of computational ship hydrodynamics for these problems, general direct stability assessment options appear to be limited to model tests and fast time-domain simulations. The simulations use potential flow wave-body hydrodynamic methods, and are supplemented by empirical formulations for viscous and vortex forces, which are based on model tests.

The main advantage of the current potential flow codes is that body-nonlinear, hydrostatic and Froude-Krylov forces can be computed efficiently and accurately. As a result, there is no need for the separation of restoring and exciting forces; strictly speaking, that can be done only under assumptions of linearity.

Keeping in mind that both pure loss of stability and parametric roll are largely driven by hydrostatic and Froude-Krylov forces, the fidelity of their modeling requires a serious consideration.

The evaluation of radiation and diffraction forces by a potential-flow code involves additional assumptions related to the techniques for solving the boundary-value problem. Therefore, one may expect an increase in the scatter in the results when benchmarking different codes.

Problems related to maneuvering in waves are more difficult to solve numerically than problems related to pure loss of stability and parametric roll. The hull forces in maneuvering depend on vortex phenomena and cannot be easily modeled using potential flow assumptions. Inclusion of empirically-based approximations for the effect of lifting phenomenon in potential flow codes may lead to significant errors. These errors are partially caused by double counting for wave forces that are implicitly included in the empirical data and inherently calculated by the potential code. Despite these difficulties, there has been substantial progress in the development of hydrodynamic models for maneuvering in waves (*cf*. Yen, *et al.,* 2010). Meanwhile, the modeling of ship maneuvering by a system of ordinary differential equations remains a mature and practical tool (SLF 53/3/8).

Validation remains an important problem for all tools that might be used in a regulatory framework (Reed, 2008). Additional work is needed to determine how the scatter in results may influence the application of these codes in a regulatory framework. The answer may be different for different modes of stability failure. However, this issue remains outside the scope of this paper.

Procedures

Having a numerical tool, even if it is validated, is insufficient for practical application in direct stability assessment. There must be a process for applying the tool that leads to a conclusion regarding the stability of the vessel under consideration.

The framework of the second generation intact stability criteria (Annex 2 SLF 51/4/1) calls for evaluation of the safety level for each mode of stability failure. If the safety level is expressed in the form of a long-term probability of a particular mode of failure, it creates a basis for comparison and a defendable outcome of the direct stability assessment. The importance of establishing good safety level criteria is that the level of safety of a new ship design can be judged against the safety level of an existing ship with a long history of safe operation.

Evaluation of long-term probability is straight forward (Sevastianov, 1994) if the short-term probability of failure is available. A short-term probability of failure is evaluated under the assumption that the environment can be described as a stationary stochastic process. However, calculation of this probability represents a significant challenge because a stability failure is, fortunately, a rare event. Thus, the estimate of the probability of failure by direct counting is impractical. The calculation of short-term probability of ship stability failure is defined in Annex 2 of SLF 51/4/1 as the problem of rarity. Addressing the problem of rarity requires application of special extrapolation procedures. Each mode of failure may require a specific extrapolation procedure that suits the particular physics of the phenomenon.

CONCLUSIONS

The objective of this paper is to describe the current state of IMO's development of second generation intact stability criteria. Following the completion of the 2008 IS code, the SLF Sub-Committee focused on new criteria that would address the dynamic stability failures not yet covered, including pure loss of stability, parametric roll, and broaching-to.

The concept of the second generation intact stability criteria is based on a multi-tiered evaluation process. Because the direct stability assessment of ship-stability performance may incur substantial additional design analysis expense, a vulnerability check needs to be performed first, to exclude cases where the modes of stability failure are not a concern. Vulnerability checks are performed at two levels to ensure simplicity and prevent unnecessary conservatism. The level 1 vulnerability check is simple, but conservative, while the level 2 is less conservative, but involves more calculations.

The level 1 vulnerability criteria for pure loss of stability is based on geometry of the hull, reflecting how dramatic changes of waterplane increase the likelihood for stability failure. The level 2 vulnerability check is performed with the GZ curve changing in waves, using different parameters as the criteria.

For parametric roll, the level 1 vulnerability criteria is based on the simplest model of parametric resonance—the Mathieu equation. Two conditions are used: the magnitude of stability changes in waves, and the encounter-frequency condition based on ship-service speed. The level 2 vulnerability criterion is based on the roll response under conditions of parametric resonance.

The vulnerability criteria for broaching-to focuses on surf-riding, as the latter is usually a pre-requisite for broaching-to. The level 1 criterion is formulated as simple conditions for service speed in terms of Froude number and vessel length. The level 2 criterion is based on the threshold speed for surf-riding under any initial conditions.

The next objective in the development of the second generation intact stability criteria is defining the requirements and procedures necessary for direct assessment. This is a formidable task. Not only must the most advanced technologies available be used, but they also need to be available world wide

At this moment, advanced potential-flow hydrodynamic codes with empirical models for lifting and viscous forces seem to be the most appropriate tools for predicting pure loss of stability and parametric roll. Broaching-to is best modeled with a system of ordinary differential equations until more advanced hydrodynamic codes gain enough maturity for this application.

Development of validation procedures for time-domain simulation tools is another difficult, but absolutely necessary task. As direct stability assessment is meant to be done under

realistic conditions, the stochastic nature of the environment needs to be fully considered. This means that stability failures must be regarded as random events and, since they are rare, the problem of rarity needs to be addressed with a set of appropriate probabilistic extrapolation procedures. Development and verification of these procedures is just as important as the development and validation of numerical tools.

Also, an additional mode of intact stability failure, excessive accelerations, needs to be addressed with suitable vulnerability criteria and direct stability assessment methods.

Once the criteria development is complete, two more stages will be needed. First, standards or acceptance boundaries must be established for the various criteria. This task will involve agreeing on socially acceptable risks of maritime activity. While this problem has been tackled in other fields of engineering, it has not yet been adequately addressed as far as intact stability is concerned.

Second, issues of implementation of the second generation intact stability regulations will need to be addressed. Implementation will rely on careful testing of the new criteria and a comprehensive analysis of the impact of new regulations on exiting and future fleets.

DISCLAIMER

The views and opinions expressed in this paper are solely and strictly those of the authors and do not necessarily reflect those of any organizations with which the authors have been associated, the national delegations in which the authors may participate, or the International Maritime Organization's working and correspondence groups on intact stability.

ACKNOWLEDGMENTS

Part of this work was supported by the USCG Office of Design and Engineering Standards, under the supervision of Mr. J. Sirkar. Some of the methods applied were based on results of research funded by the Office of Naval Research, under the supervision of Dr. L. P. Purtell. This support is greatly appreciated.

Part of this work was supported by a Grant-in Aid for Scientific Research of the Japan Society for Promotion of Science (No. 21360427). It was partly carried out as a research activity of the Stability Project of the Japan Ship Technology Research Association in the fiscal year of 2010 and funded by the Nippon Foundation. The authors express their sincere gratitude to the above organizations.

Further, the authors thank Mr. Ole Hympendahl who performed certain validation work that provided an independent check of procedures and criteria proposed.

The authors are grateful to both Dr. Art Reed and Ms. Suzanne Reed for their detailed editing that has greatly improved clarity and readability of the text.

REFERENCES

ABS (2004) *Guide for the Assessment of Parametric Roll Resonance in the Design of Container Carriers*, American Bureau of Shipping, Houston, TX, 70 p.

BASSLER, C. C., V. Belenky, G. Bulian, A. Francescutto, K. Spyrou, N. Umeda (2009) A Review of Available Methods for Application to Second Level Vulnerability Criteria. *Proc. 10th Int'l Conf. Stability of Ships & Ocean Vehicles (STAB '09)*, St. Petersburg, Russia, pp. 111–128.

BASSLER, C. C., R. Miller, A. M. Reed & A. Brown (2011) Considerations for Bilge Keel Force Models in Potential Flow Simulations of Ship Maneuvering in Waves. *Proc. 12th Int'l Ship Stability Workshop,* Washington, DC, pp. 291–307.

BECK, R. F. & A. M. Reed (2001). Modern computational methods for ships in seaway. *Trans. SNAME*, **109**:1–48.

BELENKY, V. L., *ed.* (2011) *Proc. 12th Int'l Ship Stability Workshop*, Washington, DC, viii+420 p.

BELENKY, V. & C. Bassler (2010) Procedures for Early-Stage Naval Ship Design Evaluation of Dynamic Stability: Influence of the Wave Crest. *Naval Engineers* J., **122**(2):93–106.

BELENKY, V., J. O. de Kat & N. Umeda (2008) Towards Performance-Based Criteria for Intact Stability. *Marine Tech.,* **45**(2):101–123.

BELENKY, V. L. & N. B. Sevastianov (2007) *Stability and Safety of Ships: Risk of Capsizing* (2nd ed.). SNAME, Jersey City, NJ, xx+435 p.

BELKNAP, W. F. & A. M. Reed (2010) TEMPEST — A New Computationally Efficient Dynamic Stability Prediction Tool. *Proc. of 11th Int'l Ship Stability Workshop,* Wageningen, the Netherlands, pp. 185–197.

BISHOP, R. E. D. & Price, W. G. (1978) On the truncation of spectra. *Int'l Shipbuilding Prog.,* **25**:3–6.

BRUNSWIG, J. & R. Pereira (2006) Validation of Parametric Roll Motion Predictions for a Modern Containership Design. *Proc. 9th Int'l Conf. Stability Ships & Ocean Vehicles ('06),* Vol. 1, Rio de Janeiro, Brazil, pp. 157–168.

BSU (2009) Fatal accident on board the CMV Chicago Express during Typhoon "Hagupit" on 24 September 2008 off the coast of Hong Kong, *German Federal Bureau of Maritime Casualty Investigation,* Hamburg, Germany, 64 p. (in German) (available on www.bsu-bund.de)

BULIAN, G. (2004) Approximate analytical response curve for a parametrically excited highly nonlinear 1-DOF system with an application to ship roll motion prediction. *Nonlinear Analysis: Real World Applications*, **5**:725–748.

BULIAN, G. & A. Francescutto (2008) *SAFEDOR Benchmark on Parametric roll—Brief description of the Simulation Methodology Employed in the Code SHIXDOF under Development at DINMA*, Internal Technical Report, Department DINMA, U. Trieste, Trieste, Italy.

BULIAN, G. & A. Francescutto (2010) A simplified regulatory-oriented method for relative assessment of susceptibility to parametric roll inception at the early design stage. *Proc. 4th*

Int'l Maritime Conf. on Design for Safety and 3rd Workshop on Risk-Based Approaches in the Marine Industries - Part I, Trieste, Italy, pp. 93–106.

BULIAN, G. & A. Francescutto (2011) Considerations on Parametric Roll and Dead Ship Condition for the Development of Second Generation Intact Stability Criteria. *Proc. 12th Int'l Ship Stability Workshop*, Washington, DC, pp. 7–18.

DE KAT, J. O., R. Brouwer, K. McTaggart &, W. L. Thomas (1994). Intact Ship Survivability in Extreme Waves: New Criteria from Research and Navy Perspective. *Proc. 5th Int'l Conf. Stability of Ships & Ocean Vehicles (STAB '94)*, Vol. 1, Melbourne, FL, 26 p.

DEGTYAREV, A., *ed.* (2009) *Proc. 10th Int'l Conf. Stability of Ships & Ocean Vehicles (STAB '09)*. St. Petersburg, Russia, 754 p.

FRANCE, W. M, M. Levadou, T. W. Treakle, J. R. Paulling, K. Michel & C. Moore (2003). An Investigation of Head-Sea Parametric Rolling and its Influence on Container Lashing Systems. *Marine Tech.,* **40**(1):1–19.

FRANCESCUTTO, A. (2004) Intact Ship Stability—The Way Ahead. *Marine Tech.*, **41**:31–37.

FRANCESCUTTO, A. (2007) Intact Stability of Ships-Recent Developments and Trends. *Proc.PRADS '07*, Houston, TX.

GRAFF, W. & E. Heckscher (1941) Widerstands und Stabilitäts-Versuche mit drei Fischdampfermodellen. *Werft-Reederei-Hafen,* **22**:115–120.

GRIM, O.(1951) Das Schiff von Achtern Auflaufender. Jahrbuch der Schiffbautechnischen Gesellschaft, **4**:264–287.

HASHIMOTO, H. (2009) Pure Loss of Stability of a Tumblehome Hull in Following Seas. *Proc. 19th Int'l Offshore and Polar Engin. Conf.*, Vol. 3, Osaka, Japan, pp. 717-721.

HASHIMOTO, H., N. Umeda & A. Matsuda (2011) Broaching prediction of a wave-piercing tumblehome vessel with twin screws and twin rudders. *J. Marine Sci. & Tech.* 14 p. (DOI 10.1007/s00773-011-0134-1)

HAYASHI, C. (1985) *Nonlinear Oscillations in Physical Systems*, Princeton University Press, Princeton, NJ, xii+392 p.

IACS (2001) Standard Wave Data. International Association of Classification Societies, Ltd., Recommendation No. 34, Rev. 1, London, UK, 4 p.

IKEDA, Y., M. Kashiwagi & N. Umeda, *eds.* (2008) *Proc. 6th Osaka Colloquium on Seakeeping and Stability of Ships,* Osaka, Japan.

IMO (2009) International Code on Intact Stability, 2008, IMO, London, UK, v+160 p.

IMO MSC.1/Circ.1200 (2006) Interim Guidelines for Alternative Assessment of the Weather Criterion, London, UK, 17 p.

IMO MSC.1/Circ.1227 (2007) Explanatory Notes to the Interim Guidelines for Alternative Assessment of the Weather Criterion, London, UK, 23 p.

IMO MSC.1/Circ.1228 (2007) Revised Guidance for Avoiding Dangerous Situations in Adverse Weather and Sea Conditions, London, UK, 8 p.

IMO MSC.1/Circ.1281 (2008) Explanatory Notes to the International Code on Intact Stability, 2008, London, 30 p.

IMO MSC.707 (1995) Guidance to the Master for Avoiding Dangerous Situations in Following and Quartering Seas. London, UK. 14 p.

IMO Res. A.167(ES.IV) (1968) Recommendation On Intact Stability for Passenger and Cargo Ships Under 100 metres in Length, London, UK, 15 p.

IMO Res. A.562(14) (1985) Recommendation on a severe wind and rolling criterion (weather criterion) for the intact stability of passenger and cargo ships of 24 metres in length and over, London, UK, 5 p.

IMO Res. A.749(18) (1993) Code on Intact Stability for all Types of Ships Covered by IMO Instruments, London, UK, 77 p.

IMO Res. MSC.269(85) (2008) Adoption of Amendments to the International Convention for the Safety of Life At Sea, 1974, as amended, London, UK, 11 p.

IMO Res. MSC.270(85) (2008) Adoption of Amendments to the Protocol of 1988 Relating to the International Convention on Load Lines, 1966, as amended, London, UK, 2 p.

IMO SLF 48/4/12 (2005) On the Development of Performance-Based Criteria for Ship Stability in Longitudinal Waves, Submitted by Italy, IMO, London, UK, 6 p.

IMO SLF 48/21 (2005) Report to Maritime Safety Committee, London, UK, 65 p.

IMO SLF 50/4/4 (2007) Framework for the Development of New Generation Criteria for Intact Stability, submitted by Japan, the Netherlands and the United States, London, UK, 6 p.

IMO SLF 51/4/1 (2008) Report of the Intercessional Correspondence Group on Intact Stability, Submitted by Germany, London, UK, 25 p.

IMO SLF 51/INF.4 (2008) Development of Performance-Based Intact Stability Criteria, Submitted by the United States, London, UK, 2 p.

IMO SLF 51/INF.6 (2008) Research outcomes for new generation intact stability criteria. Submitted by the Royal Institution of Naval Architects (RINA), London, UK, 4 p.

IMO SLF 52/3/1 (2009) Report of the Intercessional Correspondence Group on Intact Stability, Submitted by Japan, London, UK, 19 p.

IMO SLF 52/INF.2 (2009) Information Collected by the Intercessional Correspondence Group on Intact Stability, Submitted by Japan, London, UK, 138 p.

IMO SLF 53/3/1 (2010) Report of the Intercessional Correspondence Group on Intact Stability, Submitted by Japan, London, UK, 7 p.

IMO SLF 53/3/3 (2010) Activities of the Dynamic Stability Task Group of the Society of Naval Architects and marine Engineers, Submitted by the Royal Institution of Naval Architects (RINA), London, UK, 2 p.

IMO SLF 53/3/7 (2010) Comments on Level 1 Vulnerability Criteria for Parametric Rolling, Submitted by the United States, London, UK, 5 p.

IMO SLF 53/3/8 (2010) Comments on Proposed Criteria for Surf-riding and Broaching, Submitted by Japan and the United States, London, UK, 6 p.

IMO SLF 53/3/9 (2010) Comments on documents SLF 53/3/1 and SLF 53/INF.10. Submitted by Italy, London, 4p.

IMO SLF 53/19 (2011) Report to Maritime Safety Committee, London, UK, 43 p.

IMO SLF 53/INF.8 (2010) Sample Calculations on the Level 2 Vulnerability Criteria for Parametric Roll, Submitted by Sweden, London, UK, 18 p.

IMO SLF 53/INF.10 (2010) Information Collected by the Correspondence Group on Intact Stability, Submitted by Japan, London, UK, 151 p.

IMO SLF 53/WP.4 (2011) Report of the Working Group (Part 1), London, UK, 20 p.

JENSEN, J. J. (2007) Efficient estimation of extreme non-linear roll motions using the first-order reliability method (FORM). *J. Marine Sci. & Tech*, **12**:191-202.

KAN, M. (1990) A Guideline to Avoid the Dangerous Surf-riding. *Proc. 4th Int'l Conf. Stability of Ships & Ocean Vehicles*, University Federico II of Naples, Naples, Italy, pp. 90–97.

KEMPF, G. (1938) Die Stabilitätsbeanspru-chung der Schiffe durch Wellen und Schwingungen. *Werft-Reederei-Hafen*, **19**:200–202.

KOBYLINSKI, L. K., *ed.* (2009) *Proc. Int'l Workshop on Dynamic Stability Consideration in Ship Design*, Foundation for Safety of Navigation and Environment Protection, Ilawa, Poland. (www.ilawashiphandling.com.pl/workshop2009/workshop2009.htm)

KOBYLINSKI, L. K. & S. Kastner (2003) *Stability and Safety of Ships: Regulation and Operation*. Elsevier, Amsterdam, 454 p.

KROEGER, H-P (1986) Rollsimulation von schiffen im seegang. *Schiffstechnik*, **33**:187–216.

LIN. W. M. & D. K. P. Yue (1990) Numerical Solutions for Large Amplitude Ship Motions in the Time-Domain. *Proc. 18th Symp. of Naval Hydro.*, Ann Arbor, MI, pp. 41–66.

LONGUET-HIGGINS, M. S. (1957) The Statistical Analysis of a Random, Moving Surface. *Phil. Trans. Royal Soc. London, A*, **249**(962):321–387.

LONGUET-HIGGINS, M. S. (1976) On the Nonlinear Transfer of Energy in the Peak of a Gravity-Wave Spectrum: A Simplified Model. *Proc. Royal Soc. London A*, **347**:311–328.

LONGUET-HIGGINS, M. S. (1983) On the Joint Distribution of Wave Periods and Amplitudes in a Random Wave Field. *Proc. Royal Soc. London A*, **389**:241–258.

LONGUET-HIGGINS, M. S. (1984) Statistical Properties of Wave Groups in a Random Sea State. *Phil. Trans. Royal Soc. London, A*, **312**(1521):219–250.

MAKOV, Y. (1969) Some Results of Theoretical Analysis of Surf-riding in Following Seas. *Trans. Krylov Soc.*, Leningrad, **126**:124-128. (in Russian)

MARITIME New Zealand (2007) Incident Report Heavy Weather/Cargo Shift Aratere 3 March 2006. Maritime New Zealand Investigation Report 06-201, vi+57 p.

MATUSIAK, J. (2000) Two-stage Approach to Determination of Non-linear Motions of ship in Waves. *Proc. 4th Osaka Colloquium on Seakeeping Performance of Ships*, Osaka, Japan.

NEVES, M. A. S., J. E. M. Vivanco & C. A. Rodríguez (2009) Nonlinear Dynamics on Parametric Rolling of Ships in Head Seas. *Proc. 10th Int'l Conf. Stability of Ships & Ocean Vehicles*, St. Petersburg, Russia, pp. 509–520.

OH, I. G., A. H. Nayfeh & D. T. Mook (2000) A theoretical and experimental investigation of indirectly excited roll motion in ships. *Phil. Trans. Royal Soc. London.* **358**(1771):1853–1881.

PAULLING, J. R. (1961) The Transverse Stability of a Ship in a Longitudinal Seaway. *J. Ship Res.*, **4**(4):37–49.

PAULLING, J. R., S. Kastner & S. Schaffran (1972) Experimental studies of capsizing of intact ships in heavy seas. *US Coast Guard, Technical Report*, 58 p. (Also IMO Doc. STAB/7, 1973)

PAULLING, J. R., O. H. Oakley & P. D. Wood (1974) Ship motions and capsizing in astern seas. *Proc. 10th Symp. Naval Hydro.,* Boston, MA, pp. 532–549.

PAULLING, J. R., O. H. Oakley & P. D. Wood (1975) Ship capsizing in heavy seas: the correlation of theory and experiments. Paper 4.3, *Proc.1st Int'l Conf. Stability of Ships & Ocean Vehicles (STAB '75)*, Glasgow, 19 p.

PAULLING J. R. & R. M. Rosenberg (1959) On Unstable Ship Motions Resulting from Nonlinear Coupling. *J. Ship Res.*, **3**(1):36–46.

PEREIRA, R. (1988) Simulation nichtlinearer Seegangslasten. *Schiffstechnik*, **35**:173-193.

PETERS, W. S., V. Belenky & C. Bassler (2010) On Vulnerability Criteria for Righting Lever Variations in Waves. *Proc. 11th Int'l Ship Stability Workshop*, Wageningen, the Netherlands. pp. 7–16.

PETERS, W. S., V. Belenky, C. Bassler & K. Spyrou (2011) On Vulnerability Criteria for Parametric Roll and Surf-riding. *Proc. 12th Int'l Ship Stability Workshop*, Washington, DC, pp. 1–6.

RAHOLA, J. (1939) *The Judging of the Stability of Ships and the Determination of the Minimum Amount of Stability* Especially Considering the Vessel Navigating Finnish Waters. PhD Thesis, Technical University of Finland, Helsinki, viii+232 p.

REED, A. M. (2008) Discussion of: Belenky, V., J. O. de Kat & N. Umeda (2008) Towards Performance-Based Criteria for Intact Stability. *Marine Tech.,* **45**(2):122–123.

RICE, S. O. (1944/45) Mathematical Analysis of Random Noise. *Bell System Techn J.*, **23**(3):282–332, **24**(1):46–156.

SADAT-HOSSEINI, H., P. Carrica, F. Stern, N. Umeda, H. Hashimoto, S. Yamamura & A. Mastuda (2011) CFD, system-based and EFD study of ship dynamic instability events: Surf-riding, periodic motion, and broaching. *Ocean Engin.*, **38**:88–110.

SANCHEZ, N. E. & A. H. Nayfeh (1990). Nonlinear rolling motions of ships in longitudinal waves. *Int'l Shipbuilding Prog.*, 37(411):247–272.

SCHREUDER, M. (2005) Time Simulation of the Behaviour of Damaged Ships in Waves. Department of Shipping and Marine Technology, Chalmers University of Technology, Göteborg, Sweden, 49 p.

SEVASTIANOV, N. B. (1994) An Algorithm of Probabilistic Stability Assessment and Standards. *Proc. 5th Int'l Conf. Stability of Ships & Ocean Vehicles (STAB '94)*, Vol. 5, Melbourne, FL, 12 p.

SHIGUNOV, V. (2009) Operational Guidance for Prevention of Container Loss**.** *Proc. 10th Int'l Conf. Stability of Ships & Ocean Vehicles (STAB '09)*, St. Petersburg, Russia, pp. 473–482.

SHIGUNOV, V. & R. Pereira (2009) Direct Assessment Procedure and Operational Guidance for Avoidance of Cargo Loss and Damage on Container Ships in Heavy Weather, *International Workshop on Dynamic Stability Considerations in Ship Design (DSCSD)*, 11 p. (www.ilawashiphandling.com.pl/workshop2009/workshop2009.htm)

SHIGUNOV, V., H. Rathje, O. El Moctar & B. Altmayer (2011) On the Consideration of Lateral Accelerations in Ship Design Rules. *Proc. 12th Int'l Ship Stability Workshop*, Washington, DC, pp. 27–36.

SÖDING, H. (1982) Leckstabilität im Seegang. Report No. 429, Institut für Schiffbau, Hamburg, Germany, 69 p.

SPANOS, D. & A. Papanikolaou (2006) Numerical Simulation of Parametric Roll in Head Seas. *Proc. 9th Int'l Conf. Stability of Ships & Ocean Vehicles (STAB '06),* Vol. 1, Rio de Janeiro, Brazil, pp. 169–180.

SPYROU, K. J. (1996) Dynamic Instability in Quartering Seas: The Behavior of a Ship During Broaching. *J. Ship Res.*, **40**(1):46–59.

SPYROU, K. J. (1997) Dynamic Instability in Quartering Seas-Part III: Nonlinear Effects on Periodic Motions. *J. Ship Res.*,**41**(3):210–223.

SPYROU, K. J. (2005) Design Criteria for Parametric Rolling. *Oceanic Engin. Int'l*, **9**(1):11–27.

SPYROU, K. J. (2006) Asymmetric Surging of Ships in Following Seas and its Repercussion for Safety. *Nonlinear Dynamics*, **43**:149–172.

ST. DENIS, M. (1980) Some Comments on Certain Idealized Variance Spectra of the Seaway Currently in Fashion. *J. Ship Res.,* **24**(4):271–278.

THEMELIS, N. & K. J. Spyrou (2007) Probabilistic Assessment of Ship Stability. *Trans. SNAME,* **117**:181–206**.**

UMEDA, N., S. Izawa, H. Sano, H. Kubo & K. Yamane (2011) Validation & Verification on Draft New Generation Intact Stability Criteria. *Proc. 12th Int'l Ship Stability Workshop*, Washington, DC, pp. 19–26.

UMEDA, N., M. Shuto & A. Maki (2007) Theoretical Prediction of Broaching Probability for a Ship in Irregular Astern Seas. *Proc. 9th Intl. Ship Stability Workshop*, Hamburg, Germany, 7 p.

UMEDA, N. & S. Yamamura (2010) Designing New Generation Intact Stability Criteria on Broaching Associated with Surf-Riding. *Proc. 11th Int'l Ship Stability Workshop*, Wageningen, the Netherlands, pp. 17–25.

WALREE, F. van, *ed.* (2010) *Proc. 11th Int'l Ship Stability Workshop*, Wageningen, the Netherlands.

WATANABE, Y. (1934) On the Dynamic Properties of the Transverse Instability of a Ship due to Pitching. *J. Society of Naval Arch. Japan*, **53**:51–70. (in Japanese)

YEN, T.-G., S. Zhang, K. M. Weems & W.-M. Lin (2010) Development and Validation of Numerical Simulations for Ship Maneuvering in Calm Water and in Waves. *Proc. 28th Symp. Naval Hydro.*, Pasadena, CA, 28 p.

APPENDIX: TRANSITION-BASED BOUNDARY FOR PARAMETRIC ROLL

In principle, the effect of transients on the initiation of parametric roll can be incorporated into the frequency condition. Using the theoretical background in Hayashi (1985), following Spyrou (2005), transient effects for conditions that are close to ω_e, but not necessarily equal to $2\omega_m$, were used in SLF 53/3/9 and in Bulian & Francescutto (2011).

As a demonstration, the solution of the roll equation represented by Equation (13) is considered for a specific pair of initial conditions that makes the arbitrary constant, C_1, equal to zero (this leads to a theoretical "worst case" solution) with a very simple exponential growth of the envelope:

$$\phi(t) = C_2 e^{-\delta t} e^{-\kappa\frac{\omega_e}{2}t} \sin\left(\frac{\omega_e}{2}t + \varepsilon\right)$$

Starting from this form of the solution, it is possible to determine the magnitude of parametric excitation corresponding to a specified amplification factor, f, in n oscillations. Assuming that $\delta/\omega_m << 1$, such parametric excitation can be approximated as:

$$h = 2\sqrt{\left(1 - \frac{1}{4}\frac{\omega_e^2}{\omega_m^2}\right)^2 + \left(\frac{\delta + \delta_T}{\omega_m}\right)^2 \left(\frac{\omega_e}{\omega_m}\right)^2}, \qquad (44)$$

where δ_T is an additional "allowance" for the transient effect defined as:

$$\delta_T = \frac{\ln(f)\,|\,\omega_e\,|}{4\pi n} \qquad (45)$$

By comparing Equation (44) with Equation (25), one can see that the difference between them is the transient effect. This effect is shown in Figure 18; the transition boundary shows the combinations of parametric excitation and frequency ratio, where the parametric roll grows faster than the specified values

given the specific initial conditions. The initial conditions are the reason why the "transition curve" in Figure lies below the boundary of the criterion (21) since it represents a "theoretical worst case scenario."

In the particular case of $\omega_e = 2\omega_0$, according to Equations (44) and (45) we obtain:

$$h = 2\frac{\ln(f)}{\pi n} + \frac{4\delta}{\omega_m}$$

Indeed, while the condition of Equation (21) is based on a particular pair of initial conditions (deemed to be realistic), the curve specified by Equation (44), and as represented in Figure, represents a "theoretical worst case" scenario.

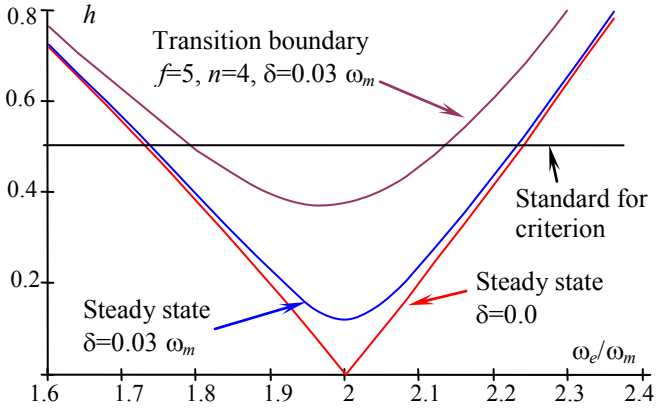

Figure 18. Effect of Transient Behavior on the Boundary for Parametric Roll